Department of Biomedical Sciences

University of Veterinary Medicine Vienna

Institute of Physiology, Pathophysiology and Biophysics
Unit of Physiology and Biophysics
(Univ.-Prof. Dr.med. Elena E. Pohl)

Influence of ketogenic diets and fasting on the expression of *ucp3*.

Bachelor thesis

University of Veterinary Medicine Vienna

Submitted by

Aleksander Szarzynski

01607461

Vienna, June 2020

Supervisor: Dr.rer.nat. Felix Locker
Univ.-Prof. Dr.med. Elena E. Pohl

Acknowledgments

At first, I would like to express my gratitude to my supervisor Univ.-prof. Dr. med. Elena E. Pohl, for giving me the opportunity to carry out my bachelor thesis in her department. Thank you for helping, correcting and consulting me during this work. The combination of being employed at the institute, but also working on an independent thesis greatly increased my confidence, experience and growth as the scientist I am today.

I would especially like to thank my second supervisor Dr.rer.nat. Felix Locker, who guided and taught me from the beginning and had the biggest influence on my development. He is the person who supported, sacrificed spare time, patiently worked and helped me every step of the way.

I am also grateful to Dipl.-Ing. Dr.rer.nat. Sasgary Soleman who shared his knowledge on primers with me and always helped me whenever I had a question.

I would like to thank both, MSc. Sarah Bardakji and MSc. Taraneh Beikbaghban, for teaching me a variety of methods and techniques, but also for your support in my day to day work.

I also like to thank Bakk. Martin Hofer for teaching and consulting me about technical devices at Vetcore.

I also thank Dipl.-Biol. Dr. rer. nat. Duvigneau Catharina for reviewing my thesis and giving me extensive feedback.

Lastly, I thank all other colleagues at the institute of physiology, pathophysiology and biophysics for being kind and having me work alongside them.

Table of content

1. Introduction

1.1 Obesity

Obesity is a major contributor to increased health problems, disease development and shortened lifespan in a population. With obesity cases gradually increasing there is an acute need for new therapies, but also in the understanding of regulatory pathways of diets and fasting conditions and their underling metabolic pathways in order to counter this growing problem of western civilisation (Finkelstein et al 2012). Obesity is caused due to an imbalance between the energy intake and energy consumption within an individual. With a higher energy intake, the body stores this energy in form of fat for later use when food is not available. What originally prevented our ancestors from starvation is becoming obsolete in western civilisations due to food oversupply. With continuous food oversupply these energy reserves reach a pathological threshold. However, a very recent study also suggests a genetic involvement in obesity as the human anaplastic lymphoma kinase (ALK) gene was shown to be correlated with obesity in humans and mice by adrenergic stimulation of the adipose organ via the hypothalamus. The authors propose ALK as a thinness gene (Orthofer et al 2020). In addition, obesity is a comorbidity factor of diseases such as cardiovascular diseases, diabetes, or the metabolic syndrome.

1.2 Mitochondria

To further understand the misbalance of energy utilization that leads to obesity, the energy management in a cell must be investigated. Mammalian eukaryotic cells are constituted of many organelles. The mitochondrion is one of the most important in regard to energy handling, which is thought to have originally lived as an independent bacterial organism and now lives in a strong endosymbiont relationship within the cell. Unlike most organelles mitochondria have an inner (IMM) and outer (OMM) mitochondrial membrane, that are separated by the intermembrane space. Referred to as “the powerhouse of the cell” the mitochondria’s main role is to synthesize adenosine triphosphate (ATP) from adenosine diphosphate in its inner membrane via the electron transport chain. The energy needed for this process to function is gained from breaking down pyruvate in the Krebs cycle, acetyl-coA derived from i) fatty acid-

beta-oxidation ii) amino acids or iii) ketone bodies by the mitochondrion. ATP is the main energy source for essential biochemical functions within the cell, involved in synthesis, signalling and movement to name a few. Due to this property mitochondria play a central role in bioenergetics and metabolism in the cell (Alberts et al 2008).

1.3 Uncoupling proteins and bioenergetics

1.3.1 Uncoupling proteins

Uncoupling proteins (UCP) were originally proposed to dissipate energy as heat (Ledesma et al 2002). UCPs are members of the mitochondrial solute carrier family (SLC25) (Palmieri 2003). UCPs are embedded in the IMM and are responsible for the translocation of protons, fatty acid (FA) anions and probably other substrates (C4 metabolites) (Vozza et al 2014). The most investigated UCP is UCP1, which was first found in brown adipose tissue (BAT) of hibernating mammals, making up for around 10% of the mitochondrial protein content (Nicholls 1976, Bouillaud et al 1984). UCP1 dissipates protons through the electrochemical gradient of the IMM, which is used by the electron transport chain to resynthesise ATP (Rousset et al 2004). This process produces high amounts of heat (Nedergaard et al 2001), that keeps hibernators warm in winter (Ballinger et al 2018) and literally burns calories. Because of this and UCP1's expression in BAT, this tissue already caught interest for obesity studies (Himms Hagen et al 1979). Unfortunately, UCP1-related research has declined until the first decade of the 21 first century, until BAT was described in adults (Zingaretti et al 2009) and reintroduced to obesity studies (Cypess et al 2009). 25 years after discovery, homologs of UCP1 were identified by screening gene libraries for homology to UCP1 (Ricquier et al 2000), adding further members of uncoupling proteins to the mitochondrial transporter family (UCP2 –UCP5) (Palmieri et al 2003). This new uncoupling proteins not only differ in their distribution throughout the body, but also in their expression compared to UCP1 (Figure 1.1) (Pohl et al 2019).

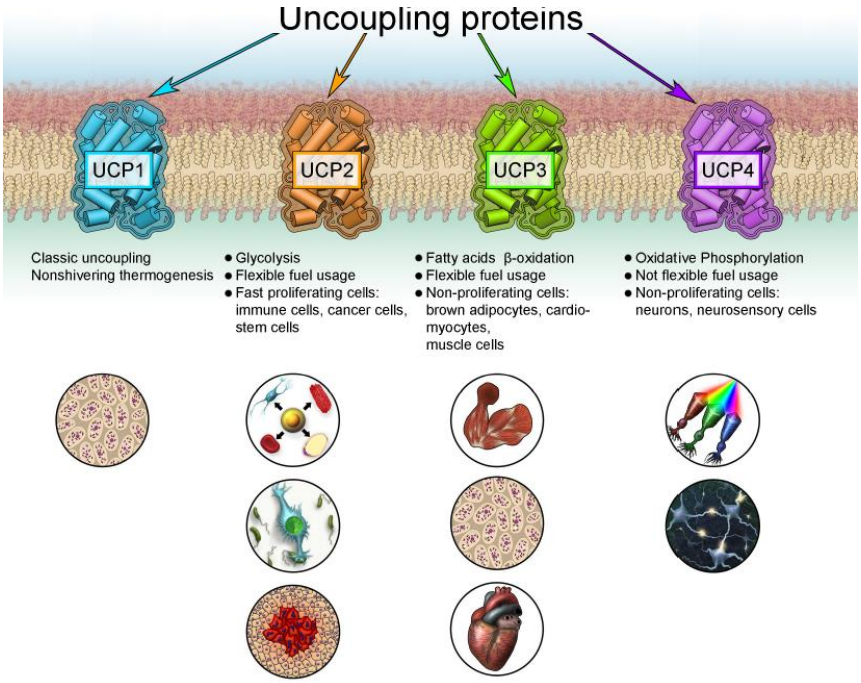

Figure 1.1 ***Proposed expression of UCP family members in different tissues throughout the mammal body and their functions. (Pohl et al 2019)***

Despite their high homology of the other uncoupling proteins to UCP1, only the latter is viewed as the only true uncoupling protein (Nicholls et al 2017). The other uncoupling proteins have various proposed functions, which are still highly debated. For example: UCP2 and UCP3 being substrate carriers (Nedergaard et al 2003) and UCP4/5 regulators of calcium movement (Ramsden et al 2012). Research has been hindered due to a lack of specific commercial antibodies for UCP subfamily members and the short lifetime of these proteins.

1.4 UCP3

1.4.1 Proposed functions

Due to the high homology of UCP3 to UCP1, it is generally proposed, that UCP3 is just a proton transporter like UCP1. In fact, proton transport occurs in UCP3, with as similar rate to UCP1 (Macher et al 2018). Interestingly, UCP3 is upregulated parallel to UCP1 upregulation during cold acclimation and is not upregulated in UCP1 KO mice, indicating that UCP3 cannot substitute UCP1 in its thermogenic function (Hilse et al 2016). Instead, UCP3 was reported to transport FA (Schrauwen and Hesselink 2007). In contrast to UCP1, UCP3 has a low expression

in BAT under cold acclimation conditions and is not assumed to have the physiological role of thermogenesis. Instead, it was proposed to transport FA for β-oxidation, as an energy source for UCP1 to achieve efficient thermogenesis (Riley et al 2016). In addition, UCP3 seems to be more active with higher long chain FA abundance (Zackova and Jezek 2001) and is upregulated when high amounts of FA are supplied. All in all, these findings reinforce the proposition, that UCP3 has a dual function of proton and FA translocation (Pohl et al 2019).

1.4.2 Expression and regulation

UCP3 was first described in 1997, by screening cDNA libraries for homologies. UCP3 has a high homology to UCP2 (72% in humans), which results in contradiction results in some experiments performed regarding UCP3's protein expression due to non-specific antibodies (Pohl et al 2019). In mice, UCP3 protein is expressed highest in BAT, heart and skeletal muscle (SkM) in this consecutive order (Hilse et al 2016). Concerning SkM, UCP3 concentrations also differ between oxidative and glycolytic muscle fibres (Russell et al 2003; Miller et al 2018). On mRNA level, the expression of *ucp3* matches with UCP3 protein manifestation, but with variations in concentration levels between mammalian tissues (Alán et al 2009). As for transcriptional regulation the proliferator-activated receptor gamma (PPARγ) is described to be a mediator of UCP3 expression during metabolic stress induced by fatty acids (Lima et al 2019). Even though UCP3 possesses an upstream open reading frame, the discrepancy between UCP3 and *ucp3* seems to be very low, suggesting that it doesn't have a high impact on UCP3's transcriptional regulations. What must be taken into consideration is the unusual short lifespan (30 min) of UCP3, when merely mRNA expression patterns are analysed. Because of this the results might not completely translate to the actual protein presence (Pohl et al 2019).

1.4.3 Influence of diets on UCP3 expression and function

Previous studies focused on the role of UCP3 in metabolism in dependence of nutritional fatty acid supplies. The diets used in the respective studies were composed of increased amounts of fat but still with substantial amounts of carbohydrates and therefore, impacting insulin signalling still significantly. This is important to mention as recent studies connected UCP3 to insulin signalling (Ochoa et al 2007) and regulation of insulin resistance during obesity in SkM (Devarshi et al 2017). Another study revealed an increase in UCP3 protein expression in

dependence of increased amounts of FA and fasting (Fisler and Warden 2006). However, no studies on UCP3 gene and protein expression were performed with ketogenic diets so far. Ketogenic diets are composed of high amounts of fat, are low in carbohydrates and moderate in protein content. Ketogenic diets have the advantage to common high fatty diets (HFD) that the amount of carbohydrates does not influence insulin signalling (Vidali et al 2014). This leads to ketogenesis of ketone bodies from FA in mitochondria of perivenous hepatocytes. Ketone bodies are transported through the bloodstream and serve as an alternative energy source, that can be processed by mitochondria via β-oxidation (Dabek et al 2020). Through the higher abundance of ketones in the bloodstream, these diets can enhance mitochondrial function and increase endogenous antioxidant defence in mitochondria.

On a molecular level sirtuin 3 (SIRT3) can be used as control for ketosis, due to its upregulation in HFD in comparison with regular diets (Miller et al 2018). It was also shown that ketogenic diets can increase the health span in mice (Roberts et al 2017). In addition, ketogenic diet feeding mimics the metabolic state of starvation and leads to a specific transcriptional program (Vidali et al 2015). Regular fatty acids can also be imported by cells, where they undergo triglyceride synthesis and can be stored in lipid droplets (LD) or transported into the mitochondrion to be further processed by β-oxidation (Bosch et al 2020). Based on the length of triglycerides which are classified regarding their carbon chain length such as medium (MCT) (≤ C10) and long chain triglycerides (LCT) (> C10). MCT derived FA can pass both mitochondrial membranes (Bach and Babayan 1982) while LCT's derived FA are activated on the mitochondrial outer membrane by the long-chain acyl- CoA synthetase but the mitochondrial inner membrane is not permeable to these acyl-CoAs. The initial activation of fatty acids, to be transported into the mitochondrion, is facilitated by transfer of an acyl-CoA group to form acylcarnitine, catalysed by carnitine palmitoyl transferase 1 (CPT1) in the OMM. Subsequently the acylcarnitine's are shuttled through the carnitine acylcarnitine translocase (CACT), located in IMM, inside the mitochondrial matrix. Finally, CPT2 which is part of this carnitine shuttle catalyses the conversion of acylcarnitine's into acyl-CoAs. Importantly, when mitochondrial fatty acid oxidation (FAO) is impaired, CPT2 catalyses the reverse reaction and converts accumulating long- and medium-chain acyl-CoAs into acylcarnitine's which are exported from the matrix to the cytosol to prevent lipotoxicity (Kerner and Hoppel 2000).

Interestingly, UCP3 was shown to have a higher upregulation in LCT supplied diets compared to diets high in MCT in SkM and heart tissue (Hoeks et al 2003; Murray et al 2011). Regularly, not all FA that enter a cell are automatically converted to energy, for a certain metabolic flexibility the cell can form LD for FA storage (Martin and Parton 2006). These LD are linked with the OMM via perilipin (PLIN) proteins (Benador et al 2018). Interestingly PLIN5 regulates the rate of FAO (Kuramoto at al 2012) and is also proposed to mediate the transport of FA through the LD membrane (Mason at al 2015).

1.1.1 Impact of diets on the expression of housekeeping genes.

Because diets have a high impact on metabolic pathways, the comparison of mRNA expression of housekeeping genes (HKG) can be rather difficult. Regularly used HKG like glycerine-aldehyde dehydrogenase (GAPDH), alpha- und beta-actin (ACTb) seem to be regulated under different metabolic conditions (Guretzky et al 2007, Moschinger et al 2019). By choosing a variety of HKG or using the most stable HKG data evaluation becomes more accurate. In general glycerine-aldehyde dehydrogenase GAPDH, that is involved in glycolysis, is used, which can be rather problematic in studies investigating glycolysis pathways. Rational approaches of HKG selection include measuring with more than one HKG and picking the least regulated in the respective experimental setting. Recent literature tested several HKG, for their stability in terms of expression strength and created a top 15 list (de Jonge et al 2007), including ribosomal protein 4 (RPL4) and ornithine decarboxylase antizyme 1 (OAZ1).

2. Hypothesis of the study

Recent literature indicated a role for UCP3 in metabolic pathways of β-oxidation, dependent on nutrient composition and fasting conditions. It was observed, that *ucp3* and corresponding transcription factors were increased in mice being fed high amounts of FA compared to other diets. However, the latter studies lacked control over carbohydrate levels, as they consisted of a substantial amount of carbohydrates. We hypothesize, that the switch from glycolysis towards ketosis and β-oxidation, by means of dietary intervention, like very low carbohydrate - ketogenic diets and fasting conditions, coincides with *ucp3* expression in tissues mainly relying on FA β-oxidation (SkM, heart, BAT) and correlates with markers of FA metabolism in mice.

2.1 Aim of the study

In this study we aimed to investigate mRNA levels of *ucp3* in murine BAT, SkM, heart, and liver of mice fed different types of diets. These diets differed in FA concentrations, calorie restrictions and fasting timeframes. To reveal the involvement of *ucp3* in FAO pathways we determined the gene expression of the master regulator of FAO peroxisome proliferative activated receptor gamma (*ppargγ*), perilipin 5 (*plin5*) which is highly expressed in oxidative tissues and regulates lipolysis of LD, carnitine-acylcarnitine-translocase (*cact*) and carnitine palmitoyl transferase 1a / 1b (*cpt1a* / *cpt1b*), being key enzymes in the transport of FA inside the mitochondria and glucose transporter 4 (*glut4*). We used ribosomal protein l4 (*rpl4*), glyceraldehyde-3-phosphate dehydrogenase (*gapdh*), actin beta (*actb*) and ornithine decarboxylase antizyme 1 (*oaz1*) as HKG to normalize the gene expression of *ucp3*. Further, we used sirtuin 3 (*sirt3*) as a positive control for induced ketosis and the voltage-depended anion carrier (*vdac*) as an indicator for the amount of mitochondria.

3. Material and methods

3.1 Material

Regular laboratory equipment, chemicals, reagents and plates that were used in this work, were supplied by VWR, Falcon, Eppendorf, Agrar-Alkohol, Roth, AppliChem and Analytikjena.

Table 3.1 ***Mice and food***

Name	Diet	Company
C57BL/6NRJ	/	/
V153xR/M-H auto	SD-CR, CR, IF	ssniff
S9139-E028	SD	ssniff
S9139-E025	LCT	ssniff
S9139-E032	LCT/MCT	ssniff

Diets can differ from the original product because some were individually prepared for the study by ssniff. Products with multiple diets had variations within this one product for each individual diet (fasting diets not included). (see 3.2.1)

Table 3.2 ***Kits, solvents***

Name	Company
peqGOLD TriFast	VWR
DNase I, RNase-free	Thermo Scientific
Glycogen	Thermo Scientific
High-Capacity cDNA Reverse Transcription Kit	Applied Biosystems
RiboLock RNase Inhibitor	Thermo Scientific
Luna	New England Biolabs
SYBR Safe DNA Gel Stain	Thermo Scientific
Bromophenol blue	Sigma-Aldrich
Hyperladder	Thermo Scientific

Table 3.3 Primer

Primer	Direction	Sequence 5'–3'	Amplicon length [bp]	GC [%]	Tm [°C]	Intron length [bp]	Amplicon length [bp]	Slope	Intercept	Range	Efficiency	Company
Ucp3	forward	TTGGCTAGACGCACAGCTTCC	21	57.1	67.8	890	73	3,322	25,805	33,75	99,99	Microsynth
	reverse	TGGAGGTCCGAGGAGAGAGC	20	65	67.8							Microsynth
Glut4	forward	TCTGACGTAAGGATGGGGAACC	22	54.6	66.6	438 + 109	178	3,336	26,959	36,28	99,42	Microsynth
	reverse	CCAGGACCTTGCCTACCCAG	20	65	67.2							Microsynth
Cpt1b	forward	CTCCGCTCGCTCATTCCGC	19	68.4	68.4		200					Microsynth
	reverse	TGCCATTCTTGAATCGGATGAACT	24	41.7	65.8							Microsynth
Cpt1a	forward	ACTCCGCTCGCTCATTCCG	19	63.2	67.3	25814	129	3,236	26,562	31,46	103,71	Microsynth
	reverse	CATGGCTCAGGCGGAGATCG	20	65	67.8							Microsynth
Cact	forward	GCAGACGAGCCGAAACCCAT	20	60	68	7433	109	3,208	23,144	23,27	104,99	Microsynth
	reverse	GTCGGACCTTGACCGTGTCC	20	65	67.6							Microsynth
Plin5	forward	GCTCTGCACCCAGGGATCTG	20	65	67.7	304	119	3,393	26,574	34,9	97,12	Microsynth
	reverse	GGCGCTAGGGTGGTGTCTTC	20	65	67.8							Microsynth
Pparγ2	forward	GAGACCAACAGCCTGACGGG	20	65	67.7	78469	99	3,355	28,74	35,84	98,65	Microsynth
	reverse	CACCGCTTCTTTCAAATCTTG	21	42.9	61							Microsynth
Rpl4	forward	GTATGGCACTTGGCGGAAGG	20	60	66.3	243	124	3,273	21,075	29,87	103,89	Microsynth
	reverse	TGCTCGGAGGGCTCTTTGG	19	63.2	67.2							Microsynth

Primer	Direction	Sequence 5'–3'	Amplicon length [bp]	GC [%]	Tm [°C]	Intron length [bp]	Amplicon length [bp]	Slope	Intercept	Range	Efficiency	Company
Oaz1	forward	CACCATGCCGCTTCTTAGTCA	21	52.4	65.6	1331	89	3,531	21,582	32,07	91,97	Biomers
	reverse	GACCCAGGTTACTACAGCAATTAAGG	26	46.2	66							Biomers
Vdac	forward	GGACTGAGAGCGAGACCCCAT	21	61.9	68.4	12339	230	3,506	30,233	32,28	94,53	Microsynth
	reverse	GTGAAGACATCCCTGGCGGAC	21	61.9	67.9							Microsynth
Gapdh	forward	GACAAAATGGTGAAGGTCGGTG	22	50	64.8	1834	97	3,425	17,98	28,26	95,87	Biomers
	reverse	TGGCAACAATCTCCACTTTGC	21	47.6	64.7							Biomers
Actb	forward	GGCCAACCGTGAAAAGATGA	20	50	63.9	454	76	3,580	20,365	31,20	90,25	Biomers
	reverse	CAGCCTGGATGGCTACGTACA	21	57.1	66.9							Biomers
Sirt3	forward	GGCGCTTGACCCTCTAGGC	19	68.4	67.8	3617	103	3,226	27,464	32,19	95,68	Microsynth
	reverse	CTGTAACACTCCCGGACCCCA	21	61.9	68.7							Microsynth

3.2 Methods

Before using the original tissue samples from differently fed mice, all the following methods, primers, RNA and protein were pretested with mice tissue from other experiments, to check and adapt the existing protocol to its final version, which is described below. Purity, concentrations, storage conditions and further information of chemical reagents are provided by the suppliers under the given product number and are therefore not listed.

3.2.1 Experimental set up

In total 56 mice of the strain C57BL/6NRJ where used for the experiments. After birth, all mice were kept under the same conditions for twelve weeks in packs of eight at ~20 °C room temperature with a 12 h/12 h day and night cycle and fed the regular amount of needed nutrients, before being introduced to one out of seven specific diets. Listed in Table 3.4 are the diets and their nutrient composition that were available to the mice *ad libitum*.

Table 3.4 ***Nutrient composition of diets.***

	Standard diet (SD)	Standard diet calorie restricted (SD-CR)	Long chain triglycerides (LCT)	Long and medium chain triglycerides (LCT/MCT)	Calorie restricted (CR)
[MJ/kg]	15.1	12,9	> 29.7	29.7	9,7
Crude Protein %	16,1	19	8,1	8,1	14,3
Crude fibre %	10	4,9	9,9	9,9	3,7
Crude fat %	0	3,3	0	0	2,5
Crude ash %	4,4	6,4	4,4	4,4	4,8
LCT %	0,8	3,25	74,6	49,6	2,4
MCT (C8) %	0	0	0	15	0
MCT (C10) %	0	0	0	10	0
Sugar %	6	4,7	1	1	3,5
Starch %	51,2	36,5	0	0	27,4

Under fasting mimicking diet (FMD) mice fasted for four days and had a recovery time of seven days. The first two days of the fasting period mice received 50 % of their nutrients and the following two - only 10 % (Table 3.5). This whole process was repeated four times.

Table 3.5 ***Nutrient composition of fasting condition FMD.***

	7 days recovery [1/d]	Day 1 and 2 (50 %) [1/d]	Day 3 and 4 (10 %) [1/d]
[kcal/d/mouse]	13,5	6,75	1,35
Broth powder [g]	4,28	2,14	1,57
Olive [g]	9,18	4,59	0
FA [g]	0,16	0,08	0
Vegetable mix [g]	10,72	5,36	0
Hydrogel [g]	47,7	23,85	27,89
Glycerol [g]	0	0	0,22

In the intermitted fasting diet (IF) mice had repeatedly access to food for 24 h, following a fasting period of 24 h. The mice were fed with the same food as SD-CR mice (Table 3.4).
After eight weeks on one diet, SkM, heart muscle, BAT, liver and other tissue were isolated from the mice after CO_2 euthanasia and cardiac puncture. The samples were immediately shock frozen in liquid nitrogen. All animal experiments were performed by our cooperation partner (Kalina Duszka, Universität Wien) and had been approved by the national authority according to §§ 26ff. of Animal Experiments Act, Tierversuchsgesetz 2012-TVG 2012 (BMWFW-66.006/0008-V/3b/2018).

3.2.2 Sample preparation

Tissue samples ranging from 40-200 mg were stored on -80 °C and were always kept on dry ice during experiments. Approximately 60 mg of tissue was cut off and put in a 5 ml tube containing 1 ml of TriFast (VWR, Austria) reagent.

3.2.2.1 Tissue homogenisation

The homogenisation was performed under the fume hood, because of the toxicity of TriFast reagent, using an Ultra-Turrax (IKA, Austria). Before and after use, the shaft of the

homogenizer was cleaned with distilled water and twice with 70 % ethanol, in this substantial order. The sample was homogenized until all tissue was solubilized. This method was mostly used for brown adipose and liver tissue. Skeletal muscle and heart tissue being more rigid, were homogenized with FastPrep-24 (MP Biomedicals, Germany) in lysing matrix D (MP Biomedicals, Germany) tubes, with the same amounts of tissue and TriFast reagent as above. Homogenization spans of 3x 30 s with 1 min rest in between, during which the samples were kept on low temperature with a dry ice cooling adapter, were used.

3.2.2.2 TriFast RNA and protein precipitation and RNA wash

The homogenized solution was thawed and transferred into 2 ml tubes. The samples were incubated at room temperature for 5 min and then immediately put back on ice. Afterwards 200 µl chloroform, was added to each sample to achieve phase separation and vortexed vigorously until a colour shift, from pinkish to milky, appeared. The tubes were then kept at room temperature for 15 min and centrifuged with 12.000 g at 4 °C.

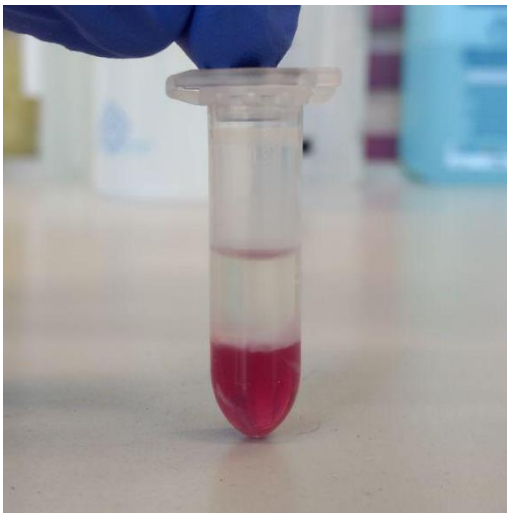

Figure 3.1 ***Phase separation****: solubilized tissue in TriFast (VWR) separates into distinct phases after addition of chloroform and subsequent centrifugation. The phases represent mRNA (colourless), DNA (white) and protein (red).*

The separated phases consist of solubilized RNA the top transparent phase, followed by the white DNA interphase in the middle and the pinkish phase at the bottom, containing the remaining biological components including proteins, were all processed as followed. RNA

containing phase was carefully transferred to a new tube and stored on ice. The interphase of DNA was discarded, and the remaining organic solution was stored at 4 °C for a maximum of one week, before being processed further for protein isolation. 500 µl of isopropanol was added to each tube containing RNA phase to start precipitation. Also 1 µl of glycogen (Thermo Scientific, Austria), which binds to RNA and turns it white for easier detection, was included. Tubes were then inverted five times, stored for 10 min at room temperature and centrifuged for 8 min with 12.000 g at 4 °C.

The isopropanol supernatant was discarded, and the remaining white pellet of mRNA washed, by adding 1 ml of 75 % ethanol subsequent vortexing. After the final step of centrifugation of 5 min with 7.500 g at 4 °C, the remaining ethanol was removed. The tubes were left open for a maximum of 10 min under a lamina hood, so that reaming traces of ethanol could evaporate, without contaminating the samples. Afterwards the dry mRNA pellet was dissolved in 60-80 µl of nuclease free water (NF-H_2O) (VWR, Austria), dependent on size, by gentle up and down pipetting and incubation at 60 °C for 10 min. 30 µl where aliquoted from each sample and stored at -80 °C.

3.2.2.3 RNA integrity

To check the mRNA quality and integrity, we tested mRNA form pre-test mice prior our main runs on TapeStation 4200 (Agilent, Austria) to determine our mRNA integrity number (RIN) (4.1).

3.2.2.4 DNAse digestion

The DNAse digestion was performed under a lamina hood, while always keeping the samples and reagents on ice, and enzymes on -20 °C cooling racks. At first the concentration of each mRNA sample was measured with NanoDrop (Thermo Scientific, Austria), in order to calculate the required volume corresponding to 4 µg of RNA. 4 µl (4 u) of DNAse I, 2 µl of 10x reaction buffer with $MgCl_2$ from DNase I, RNase-free kit (Thermo Scientific, Austria) and 4 µg of mRNA were pipetted into PCR tubes. The mixture was then filled up to a total volume of 20 µl with NF-H_2O, before being incubated at 37 °C for 30 min. In the meantime, the mRNA samples were put back into the -80 °C freezer. After the DNA digestion 2 µl of 50 mM EDTA

from the same kit were added to each sample to deactivate the DNAse I enzyme. Additionally, the samples were incubated for 10 min at 65 °C to denaturate the DNAse I enzyme.

3.2.2.5 Reverse transcription to cDNA

The reverse transcription from mRNA to cDNA was performed under a lamina hood, with the samples kept under the same conditions as mentioned before, directly after the DNAse digestion step. 4 µl of reverse transcriptase buffer, 1.6 µl of 100 mM dNTPs-mix, 4 µl of 10x reverse transcriptase random primer from High-Capacity cDNA Reverse Transcription Kit (Applied Biosystems, Germany), 0.5 µl of RiboLock RNase inhibitor (Thermo Scientific, Austria) and 5.9 µl of NF-H_2O were transferred to each sample. At the end 2 µl of the multiscript reverse transcriptase (50 U/µl), were added, summing it up to 18 µl in total for every sample. Subsequently the cDNA synthesis was performed using the following setting for temperature conditions (Table 3.6) for the thermal cycler PCR System 9700 GeneAmp (Thermo Scientific, Austria):

Table 3.6 ***Temperature conditions for reverse transcription of mRNA to cDNA***

Temperature [°C]	25	37	85	4
Time [min]	10	120	5	∞

The reverse transcription was finished when 4 °C was reached. Finally, 40 µl of NF-H_2O was added to each tube, to dilute the cDNA and all reaming protein and complex residues from previous steps, yielding 80 µl cDNA samples.

3.2.3 Primer design

All primers were designed using NCBI primer-blast (Ye at al, 2012). The whole FASTA sequence of a given protein coding region on the genomic DNA was used, as PCR template. The amplicon size was reduced for its maximum to be 190 Bp in order to achieve high amplification efficiencies, with a few exceptions being > 200 Bp if no primers could be found (Table 3.3). The primer melting temperatures (Tm) settings were increased to: min = 60 °C, Opt = 63 °C, Max = 66 °C to reduce unspecific binding probability of the primers. Also, the intron inclusion box was checked, and the organism set to *mus musculus* (taxid:10090). All other parameters were kept at default by NCBI primer-blast.

After arrival, primers (Microsynth, Austria) were solubilized in NF-H_2O according to manufacturer's instructions, leading to a final concentration of 100 µM. Afterwards 10 µl of forward and reverse primer for one unique gene were added to 980 µl NF-H_2O. These individual 1 pmol/µl primer-solutions, for every gene region were used in all following steps.

3.2.4 RT-qPCR melting temperatures and gel electrophoresis

The primer-solutions were tested on a temperature gradient (Table 3.7) in duplicates within every step, representing independent annealing temperatures. This was performed to determine the optimal annealing temperature for every primer and test whether the generated amplicons differ in length within on primer depending on temperature.

Table 3.7 ***Temperature distribution*** *for individual annealing temperatures throughout the 96 well plate, used for melting temperature determination.*

Step	1	2	3	4	5	6	7	8	9	10	11	12
Temperature [°C]	59	59.1	59.5	60	60.6	61.2	61.8	62.4	63	63.5	63.9	64

96 well plates were used, each well containing a master mix with 5 µl Luna (New England Biolabs, Germany), 2.5 µl primer-solution, 2 µl NF-H_2O and 0.5 µl cDNA gained from pooled pre-test mice heart and skeletal muscle. At first the primer solutions were pipetted; the master mix was added afterwards. The plates were sealed with 96 well transparent foil and centrifuged to remove bubbles. The RT-qPCR was run qTower3 84 (Analytikjena, Germany) with the following setup (Figure 3.2), with 100 °C lid temperature.

	4 steps	scan	°C	m:s	goto	loops	ΔT(°C)	Δt(s)	↗(°C/s)
	1		95,0	01:00	--	---	--,-	---	8,0
40x	2		95,0	00:15	--	---	--,-	---	8,0
	3		59,0-64,0	00:30	--	---	--,-	---	6,0
	4	◆	72,0	00:30	2	39	--,-	---	6,0
	5	◆	Melt	00:15					

Figure 3.2 ***RT-qPCR program setup used for melting temperature determination***

To check if the RT-qPCR worked and if the amplicons have the right size, a gel electrophoresis was performed with the PCR products.

3 g agarose were added to 110 ml TBE-buffer (89 mM Tris, 89 mM boric acid, 2 mM EDTA, 1 mM guanosine) and boiled with an open lid in a microwave, until it was transparent. 10 µl SYBR gel stain (Thermo Scientific, Austria) were added, before the gel was cast in a chamber containing a comb for loading pockets. After the gel hardened each pocket was filled with premixed 2 µl loading dye (250 g/l saccharose, 1.25 g/l bromophenol blue (Sigma-Aldrich, Austria) in TBE-buffer) and 10 µl from one well of the previous RT-qPCR. An additional pocket was used for 5 µl of ladder solution (Thermo Scientific, Austria). Noted, only wells above an annealing temperature of 60.6 °C were used and each primer-solution tested in duplicates. Bands separated with 180 V for at least 2 h and afterwards visualized using UV-illumination 256 nm using Quantum (Vilber, Germany).

3.2.5 RT-qPCR efficiency tests

Primers were checked vigorously for efficiency and occurrence of the proper amplicon size under pre-optimised annealing temperatures (4.1.1) (highest possible temperature was chosen to reduce unspecific binding of the primer). 384 well plates were used, and primer-solutions tested in triplicates for every dilution. In contrast to the RT-qPCR master mix as previously described, the amount of primer-solution was increased to 3 µl and the NF-H_2O decreased to 1.5 µl. Luna fluorescent dye (New England Biolabs, Germany) and cDNA concentration stayed the same stayed the same, representing the 1:1 dilution. In sum 11 master mixes were made with cDNA dilutions ranging from no to 1:1024. At first the primer solutions were pipetted; the master mix was added afterwards. Plates were sealed with transparent foil and spinned down to remove bubbles. Additionally, no template controls (NTC) were provided having NF-H_2O instead of cDNA to check primer-solution for contaminations. Also, reverse transcription controls (RT-), which were treated just as the pre-test RNA, but with NF-H_2O instead of multiscript reverse transcriptase, were performed. While NTC had to be performed for every primer-solution used in each run, RT- was only performed once to control and verify the required specificity of the PCR reaction process. The pipetting of the 384 well plate was performed with a pipetting robot epMotion 5075 (Eppendorf, Austria). The annealing temperature was set to 62 °C (see 4.1.1). After the lid was pre heated to 100 °C the RT-qPCR was run qTower3 84 (Analytik Jena, Germany) (Figure 3.3).

	4 steps	scan	°C	m:s	goto	loops	ΔT(°C)	Δt(s)	↗(°C/s)
	1		95,0	01:00	--	---	--,-	---	4,0
45x	2		95,0	00:15	--	---	--,-	---	4,0
	3		62,0	00:30	--	---	--,-	---	2,0
	4	◆	72,0	00:30	2	44	--,-	---	2,0
	5	◆	Melt	00:15					

Figure 3.3 ***RT-qPCR program setup for efficiency test with adjusted annealing temperature***

3.2.6 RT-qPCR of samples

After determining the of efficiency amplification for primer pairs, each cDNA was tested with every primer-solution in triplicates. 384 well plates were used. The cDNA from the experimental mouse groups was used without further dilution. Each well contained 5 µl Luna, 3 µl primer-solution, 1.5 µl NF-H_2O and 0.5 µl cDNA. NTC and RT- were tested in duplicates. The pipetting and setup (Figure 3.3) were performed just as described above.

3.2.7 Statistical analysis

Using the qPCRsoft384 software (Analytik Jena, Germany), the datasets were exported to an excel file for further calculations. First all datasets were tested for outliners using Grubbs' test. Values with a significance of $P \leq 0.05$ were considered to be outliers and excluded from further analysis. Statistical analysis was performed with GraphPad 7, using the one-way analysis of variance ANOVA with Kruskal-wallis (nonparametric statistical analysis) and Dunn's multiple comparisons test. In the ketogenic group SD was tested against LCT/MCT and LCT and significant differences (P-values) marked with: + $P \leq 0.05$, ++ $P \leq 0.01$, +++ $P \leq 0.001$ and ++++ $P \leq 0.0001$. Furthermore LCT/MCT was tested against LCT and significant differences (P-values) marked with: * $P \leq 0.05$, ** $P \leq 0.01$, *** $P \leq 0.001$ and **** $P \leq 0.0001$. Lastly in the calorie restricted and fasting group SD-CR was tested against CR, IF and FMD and significant differences (P-values) marked with: # $P \leq 0.05$, ## $P \leq 0.01$, ### $P \leq 0.001$ and #### $P \leq 0.0001$.

4. Results

4.1 RNA integrity

First, we wanted to verify that our extraction method delivers intact mRNA. The integrity of mRNA is crucial, because it was reverse transcribed into cDNA. If mRNA is too much degraded, the corresponding cDNA will not picture the mRNA present in the original tissue. In further analysis of this cDNA would yield wrong data. Because mRNA degradation already happens in the tissue, not to mention during extraction, extracted mRNA will always be degraded. How much degradation occurred is dependent on many factors, but mainly on the method and process. To test our method, we used mice tissues relevant in our study to evaluate their RIN values with the Tapestation 4200 (Agilent, Austria). RIN values in the range between eight and ten, are considered suitable for analysis of expression analyses by RT-qPCR. In the case of our four tissues of interest, this extraction method provided us with mRNA of good integrity (Figure 4.1). The RIN value determination evaluates our extraction method for one type of given tissue.

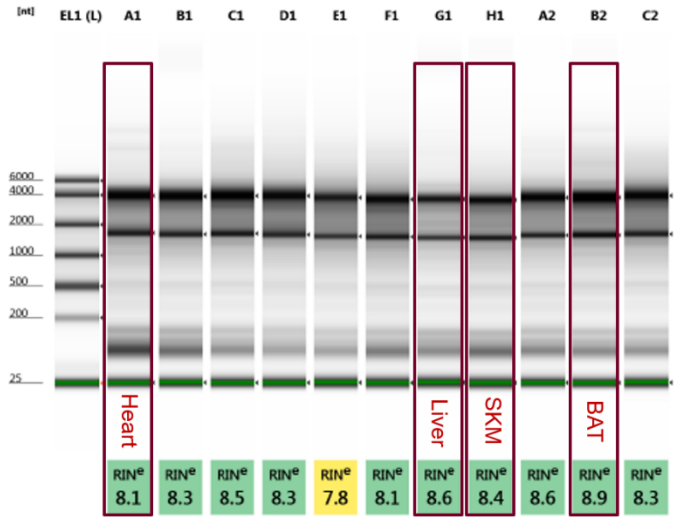

Figure 4.1 ***mRNA integrity numbers*** *(RIN) of heart, liver, skeletal muscle (SkM) and brown adipose tissue (BAT).*

4.1.1 RT-qPCR melting temperatures and gel electrophoresis

To check the primers, we performed melting temperature tests to find out their optimal annealing temperature and single amplicon production, for one gene. The melting curves of all genes (Table 3.3) showed little difference between each other, with only one peak having an offset based on the amplicon size and its GC-content (Figure 4.1, Figure 3.3). The peek for every primer's amplicon was also measured, at the approximate in silico determined melting temperature.

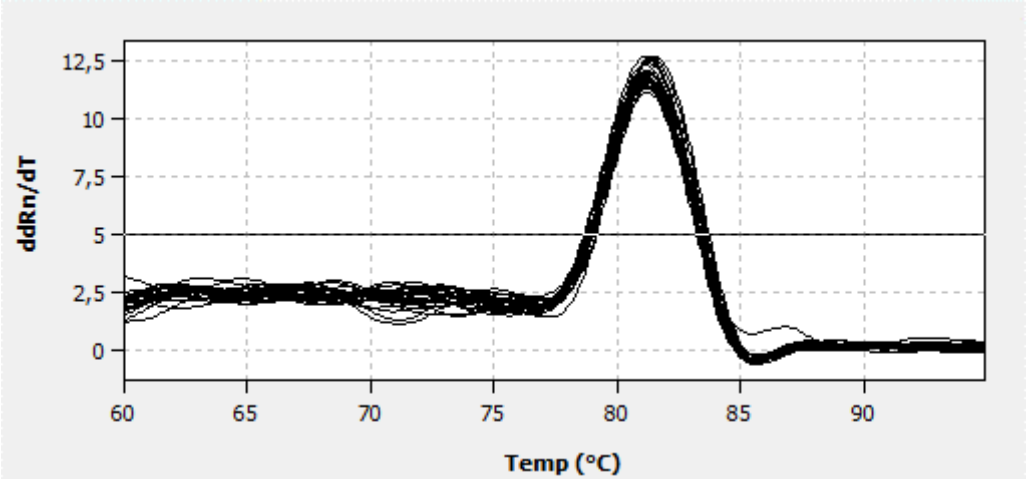

Figure 4.2 ***Example melting curve of mUCP3****, UCP3 Primer was used after RT-qPCR melting temperature determination, using pooled pre-test mice heart and skeletal muscle cDNA. One peak corresponds to one amplicon of unknow size, which can be further used and evaluated in Gel electrophoresis.*

To further confirm the reliability of the primers, the corresponding amplicons of the melting temperature test were checked via gel electrophoresis (Figure 4.3). The amplicons, shown in duplicates, can be seen on the same height as determined in silico (Table 3.3). With all primes producing amplicons even at higher temperatures, the annealing temperature for the efficiency test was set accordingly to 62 °C.

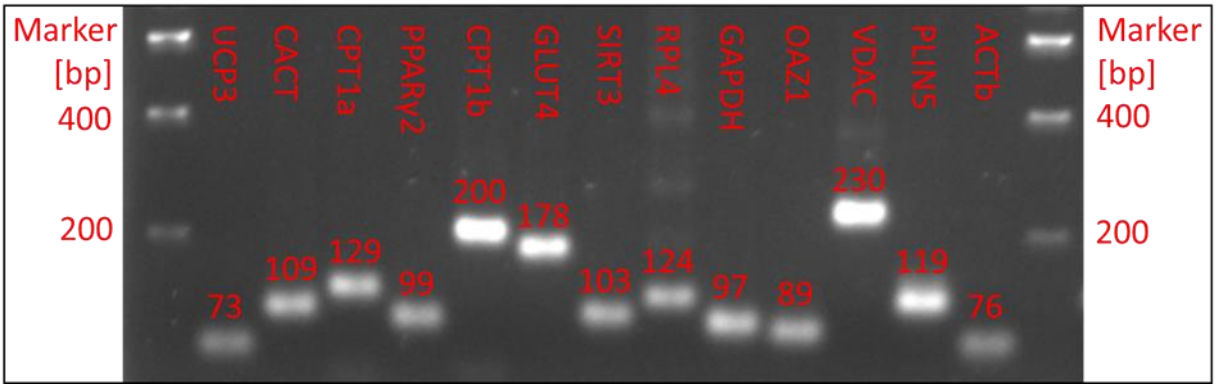

Figure 4.3 ***Gel electrophoresis of RT-qPCR amplicons*** *of relevant primers with Insilco determined amplicon sizes for reference (Table 3.3).*

4.1.2 RT-qPCR efficiency tests

To determine the efficiency for every primer, a dilution series of cDNA gathered from pre-test mouse heart and liver tissue was used. We calculated slopes, intercepts, and the primer efficiency for the corresponding genes from the efficiency tests data (Table 3.3). The cycle of quantification (ct) threshold was set to 25 and the fitted regression of the obtained measurements had to have an R-squared of at least 0.995, to be evaluated. Based on the melting curve, that was performed after the RT-qPCR, datapoints, that did not match the original amplicons Tm, were excluded. Because there are slight differences between runs and devices, the Tm can vary in a range of ± 0.5 °C from the median of all measured peeks for one primer, to still be valid. If all peeks are strongly offset by > 1.5 °C compared to all prior runs it had to be repeated. Also values that fluctuated more than ± 0.5 ct from a given triplets mean, or major outliers, were excluded. If only one value of a triplet was left matching all criteria, that specific triplet had to be repeated. The criteria for primer efficiencies was set to be between 90 and 105%. Unfortunately, CPT1b's efficiency could not be calculated and still needs to be repeated. The melting curve and fitted regression of UCP3 primer's efficiency test is shown in Figure 4.4. The values of Tm and ct match all our criteria, meaning that this primer can be used in further experiments. The same test was performed for every primer in Table 3.3 excluding CPT1b.

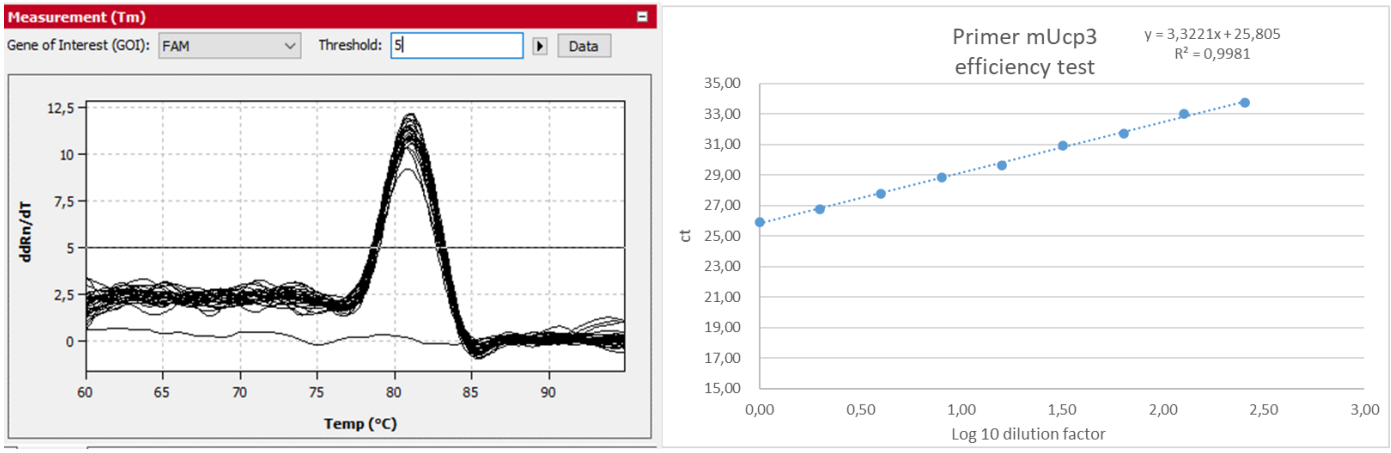

Figure 4.4 ***Representative example of first derivative melting curve with negative control (left) and regression line (right)*** *with R², slope and intercept of primer UCP3, calculated with the respective efficiency test RT-qPCR data. Tm of UCP3 matches our requirements for the Tm of UCP3's RT-qPCR melting temperature test (left). Plotting the ct values against the logarithm of the dilution series (see 3.2.5) and fitting a regression line, calculates the slope from which the efficiency of UCP3 was determined (Table 3.3) (right).*

4.1.3 Expression of *ucp3* and other genes involved in glucose-, fatty acid and lipid metabolism

With all primers tested, cDNA of BAT, SkM, heart and liver were analysed for all tissue adequate genes with RT-qPCR.

Data obtained from SkM, heart and BAT samples were normalized towards mRpl4, using the delta ct method. With this method we subtract the value for the HKG (in this case mRpl4 or mOaz1) from that of the gene of interest. For liver samples we used mOaz1, because our RPL4 primer produced errors regarding Tm in this particular tissue and therefore could not be used as normalization to mRpl4. The result was the difference between the ct of HKG and the gene of interest ct (Δct), in order to receive relative values, the $2^{-\Delta ct}$ method was used and plotted (Figures 4.5-4.8). Otherwise all described criteria regarding Tm and ct, mentioned in 4.1.2 were followed.

If stated n.d. (not detectable) experiments were performed but ct values did not reach the threshold. If nothing is indicated, data are still missing due to pandemic-related delay.

4.1.3.1 Impact of diets and fasting conditions on housekeeping genes

Beforehand, to normalize our RT-qPCR data we evaluated HKG. We observed strong changes in gene expression of commonly used HKG such as *gapdh* and *oaz1* (stable in liver only). Only the *rpl4* gene was stably expressed over all diets and tissues and therefore it was used as a primary reference gene in BAT, heart and SkM.

4.1.3.2 Gene expression in brown adipose tissue

BAT, a prominent expression site of *ucp3* (Pohl et al 2019), was investigated upon ketogenic diet feeding and fasting conditions.

Our results (Figure 4.5) show that LCT feeding decreases the expression of *glut4* and *gapdh* significantly in comparison to SD-feeding. The substitution of 35 % LCT with MCT resulted in a significant increase of *ucp3* gene expression along with other genes involved in FA-metabolism and lipid handling such as *cpt1a, cpt1b, plin5, pparγ2* and *sirt3* compared to SD-fed mice. In line with this, the LCT diet fed mice had significantly lower expression levels of *cpt1a, cpt1b, plin5, pparγ2, sirt3* and *cact* compared to the LCT/MCT diet. FMD reduced glut4 mRNA levels in BAT in comparison to the respective control diet (SD-CR), however, *gapdh* levels remained unchanged. IF-mice BAT tissue had a significantly higher expression of *plin5, sirt3, pparγ2, cact* and *vdac* in comparison to control fed mice, which is remarkable given the circumstances that mice were food deprived only for 24 h, showing the fast adaptability of the system. However, permanent caloric restriction (75% calories of SD-CR) resulted only in the downregulation of *cpt1a* and *cpt1b* in BAT, which indicates general lower nutrient circulation. The change of *glut4* and *gapdh* in LCT fed mice indicates a changed metabolism in BAT, most likely due to higher utilization of ketone bodies and FA under reduced glucose amounts. Reduced gluconeogenesis and an oversupply of energy rich FA during ketosis is regularly observed in cancer patients (Zhou et al 2007). However, our results of *ucp3* expression under LCT and LCT/MCT diets contradict literature reports (see discussion).

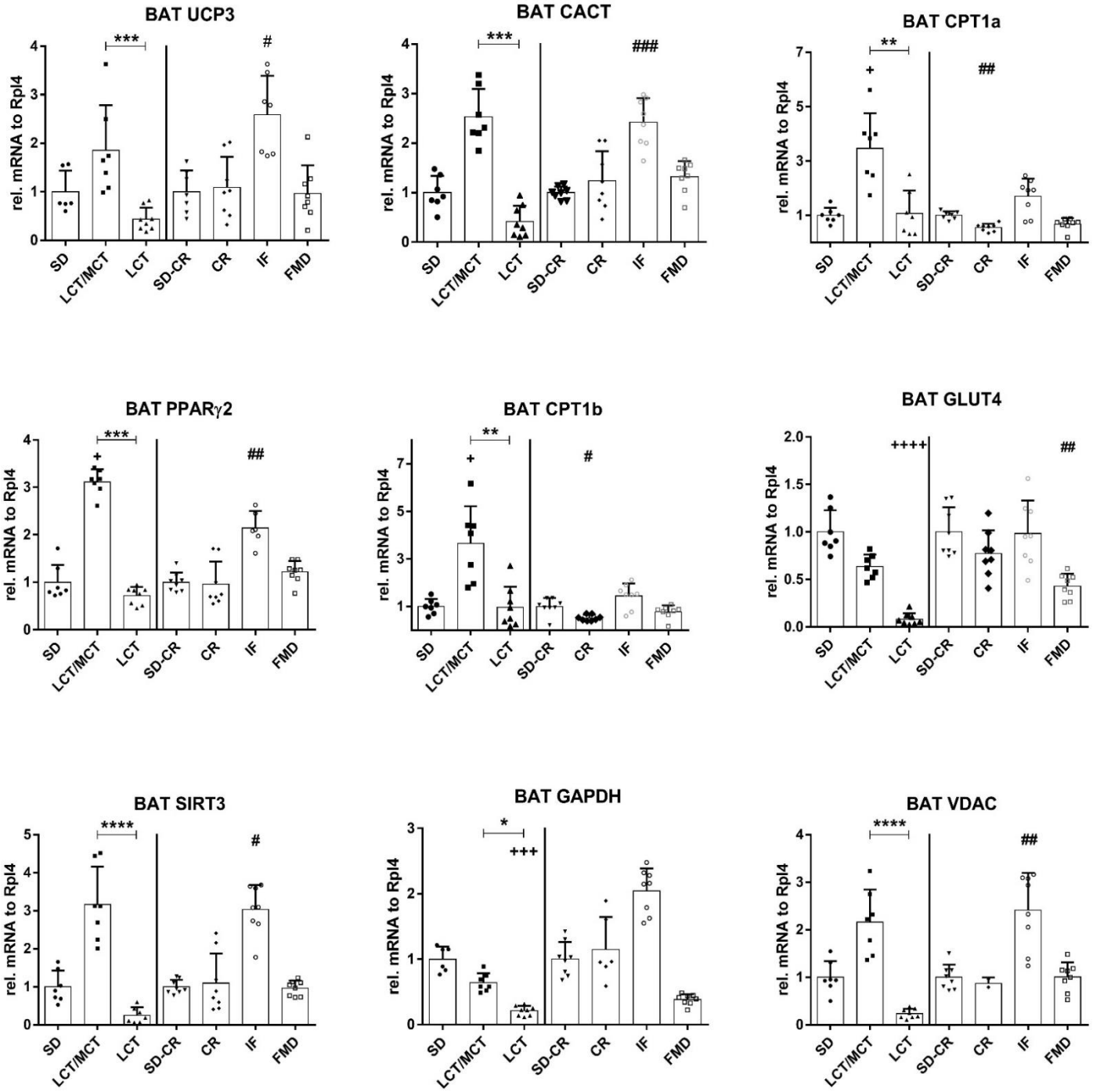

Figure 4.5 ***Molecular mRNA expression in LCT/MCT, LCT, CR, IF and FMD to the respective control diet (SD or SD-CR) in murine brown adipose tissue (BAT).*** *Relative mRNA levels of ucp3, cact, cpt1a, cpt1b, pparγ2, glut4, plin5, sirt3, gapdh and vdac normalized towards rpl4. All values are depicted as mean ± SD, n = 7-8 mice per group, one-way ANOVA and Dunn's multiple comparison, non-parametric Kruskal-Wallis. SD tested against LCT/MCT and LCT: significant differences (P-values) marked with + P ≤ 0.05, ++ P ≤ 0.01, +++ P ≤ 0.001 and ++++ P ≤ 0.0001, LCT/MCT tested against LCT: significant differences marked with * P ≤ 0.05, ** P ≤ 0.01, *** P ≤ 0.001 and **** P ≤ 0.0001, SD-CR tested against CR, IF and FMD: significant differences marked with: # P ≤ 0.05, ## P ≤ 0.01, ### P ≤ 0.001 and #### P ≤ 0.0001. LCT, long chain triglycerides; LCT/MCT, long and medium chain triglycerides; SD, standard diet; SD-CR, standard diet calorie restricted; CR, calorie restricted; IF, intermitted fasting; FMD, fasting mimicking diet.*

4.1.3.3 Gene expression in heart

As recent literature from our lab (Hilse et al 2016) indicates an important involvement of *ucp3* in murine heart metabolism we analysed *ucp3* mRNA expression in heart tissue among other metabolically important genes.

Our results (Figure 4.6) show that the heart tissue of mice, which were subjected to IF, had higher levels of *ucp3*, *cact, cpt1a, cpt1b, pparg*γ*2, plin5* and *vdac* mRNA in comparison to the control SD-CR diet. Even though insignificant an overall higher expression in *gapdh* (trend, P = 0.08) mRNA can be seen under this fasting condition. The LCT/MCT diet increased *ucp3*, *cpt1a, cpt1b, plin5, pparg*γ*2, cact, vdac* and *sirt3* mRNA levels in the heart compared to SD and in comparison to LCT fed mice the transcripts of *plin5, sirt3, gapdh, vdac, glut4, cpt1a, cpt1b* and *pparg*γ*2* were significantly higher. Interestingly, the results obtained for *ucp3* gene expression in heart are contradictory to the literature data (Montgomery et al 2013; Wang et al 2018) and are discussed in detail in the discussion section of this thesis.

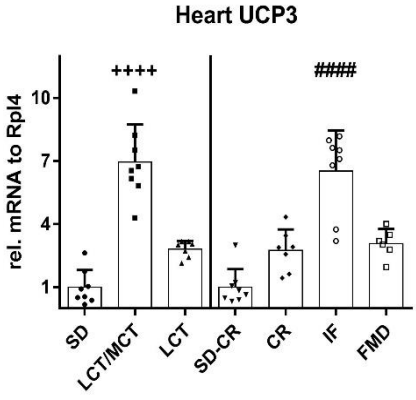

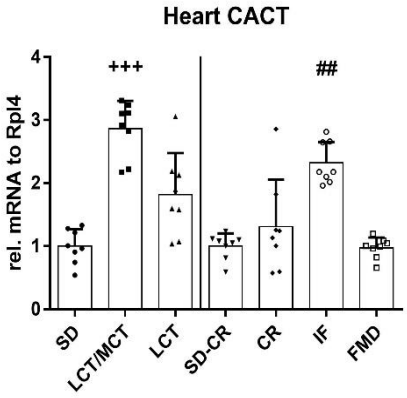

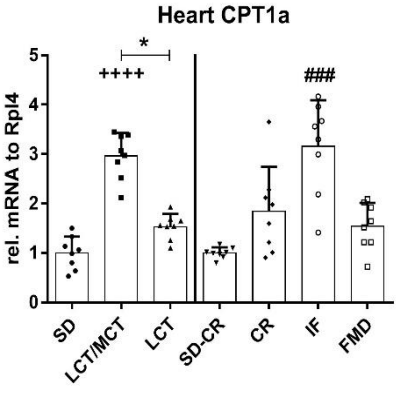

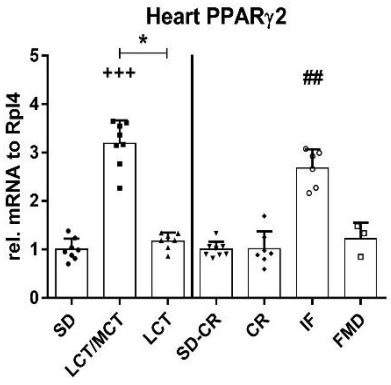

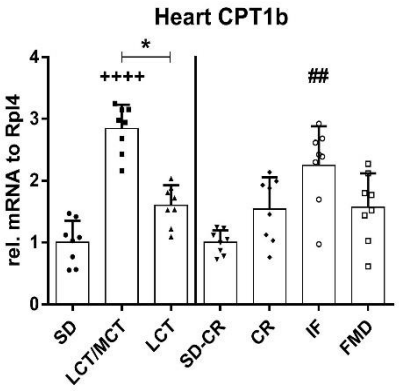

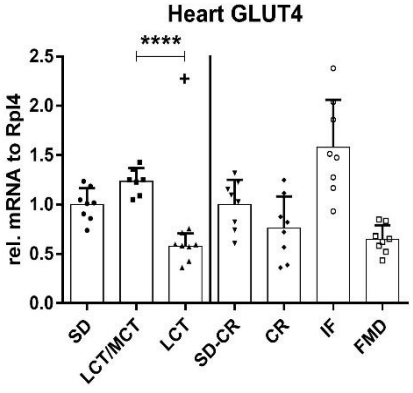

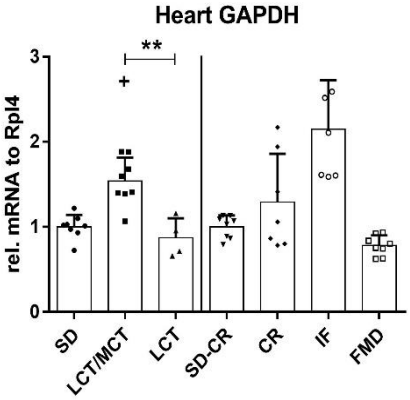

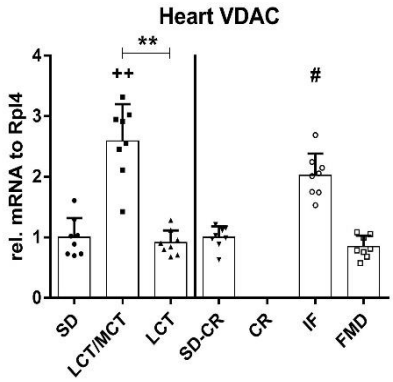

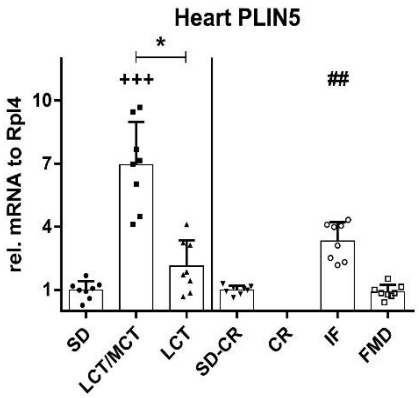

Figure 4.6 ***Molecular mRNA expression in LCT/MCT, LCT, CR, IF and FMD to the respective control diet (SD or SD-CR) in murine heart tissue.*** *Relative mRNA levels of ucp3, cact, cpt1a, cpt1b, pparγ2, glut4, sirt3, plin5, gapdh and vdac normalized towards rpl4. All values are depicted as mean ± SD, n = 7-8 mice per group, one-way ANOVA and Dunn's multiple comparison, non-parametric Kruskal-Wallis. SD tested against LCT/MCT and LCT: significant differences (P-values) marked with + P ≤ 0.05, ++ P ≤ 0.01, +++ P ≤ 0.001 and ++++ P ≤ 0.0001, LCT/MCT tested against LCT: significant differences marked with * P ≤ 0.05, ** P ≤ 0.01, *** P ≤ 0.001 and **** P ≤ 0.0001, SD-CR tested against CR, IF and FMD: significant differences marked with: # P ≤ 0.05, ## P ≤ 0.01, ### P ≤ 0.001 and #### P ≤ 0.0001. LCT, long chain triglycerides; LCT/MCT, long and medium chain triglycerides; SD, standard diet; SD-CR, standard diet calorie restricted; CR, calorie restricted; IF, intermitted fasting; FMD, fasting mimicking diet.*

4.1.3.4 Gene expression in skeletal muscle

The SkM is a known expression site for *ucp3* and it was shown to get upregulated upon HFD feeding (Fisler and Warden 2006). Therefore, we analysed SkM tissue of mice fed ketogenic diets or mice which were subjected to different fasting regimens regarding their *ucp3* mRNA among other genes involved in FAO and lipid handling.

Our results (Figure 4.7) show that the IF mouse group had higher levels of *plin5* and *cact* compared to the control SD-CR diet, indicative for LD storage and FA transport inside the mitochondria, yet, *ucp3* was not altered in this regimen. In contrast LCT/MCT feeding upregulated *ucp3*, *cpt1a, cpt1b, plin5, pparγ2, gapdh, cact, vdac* and *sirt3* mRNA levels compared with SD- and LCT- fed mice. Again, our results for *ucp3* regulation in LCT and LCT/MCT diets contradict literature reports (see discussion).

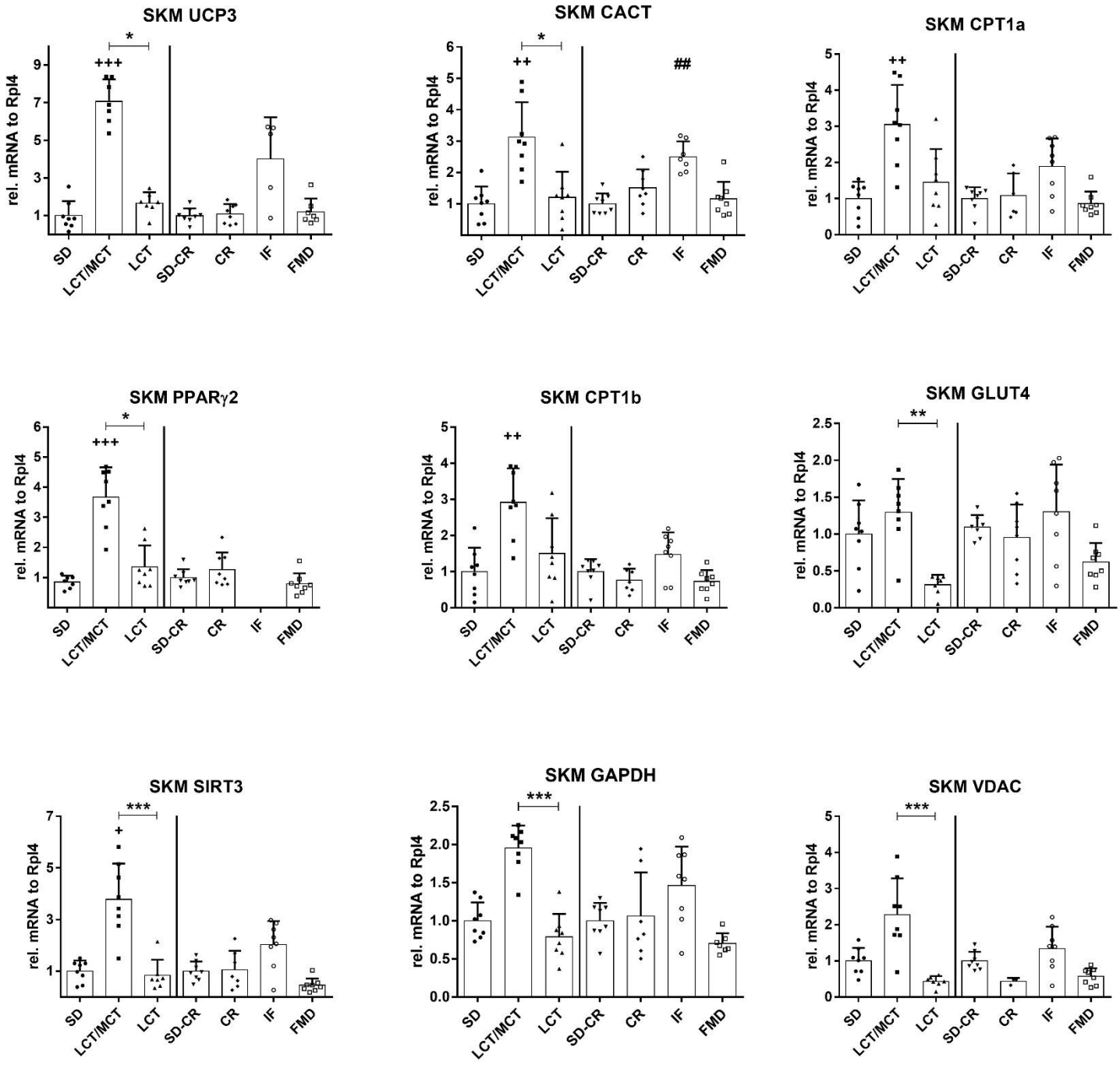

Figure 4.7 ***Molecular mRNA expression in LCT/MCT, LCT, CR, IF and FMD to the respective control diet (SD or SD-CR) in murine skeletal muscle (SKM) tissue.*** *Relative mRNA levels of ucp3, cact, cpt1a, cpt1b, pparγ2, glut4, sirt3, plin5, gapdh and vdac normalized towards rpl4. All values are depicted as mean ± SD, n = 7-8 mice per group, one-way ANOVA and Dunn's multiple comparison, non-parametric Kruskal-Wallis. SD tested against LCT/MCT and LCT: significant differences (P-values) marked with + P ≤ 0.05, ++ P ≤ 0.01, +++ P ≤ 0.001 and ++++ P ≤ 0.0001, LCT/MCT tested against LCT: significant differences marked with * P ≤ 0.05, ** P ≤ 0.01, *** P ≤ 0.001 and **** P ≤ 0.0001, SD-CR tested against CR, IF and FMD: significant differences marked with: # P ≤ 0.05, ## P ≤ 0.01, ### P ≤ 0.001 and #### P ≤ 0.0001. LCT, long chain triglycerides; LCT/MCT, long and medium chain triglycerides; SD, standard diet; SD-CR, standard diet calorie restricted; CR, calorie restricted; IF, intermitted fasting; FMD, fasting mimicking diet.*

4.1.3.5 Gene expression in liver

To evaluate if mice achieve the ketogenic state in our high fat ketogenic diets (LCT and LCT/MCT) and if fasting conditions (IF, FMD and CR) have a similar influence on the metabolism as ketogenic diets, liver tissue was examined. We have measured the mRNA expression levels of *ucp3* and important FA-metabolism related enzymes *sirt3* and *pparγ2*; carnitine translocase members *cact*, *cpt1a* and *cpt1b*; LD-associated *plin5*; glycolysis involved protein and HKG *gapdh,* and OMM protein *vdac.*

Our results (Figure 4.8) show upregulated *sirt3* and *pparγ2* levels upon LCT and LCT/MCT feeding in liver tissue. LCT, LCT/MCT and FMD based diets induce slight upregulation of gene expression of *ucp3* in liver. The LCT diet, IF and FMD conditions significantly upregulated the carnitine translocase members *cact*, *cpt1a* and *cpt1b* additionally, in LCT fed mice *Plin5* was upregulated upon LCT and LCT/MCT feeding. The HKG *gapdh* was regulated in dependence of the amount of LCT and MCT fats inside the ketogenic diets as depicted by a significantly higher expression of *gapdh* in LCT than in LCT/MCT fed mouse liver tissue. Lastly, *vdac* showed no regulation in liver tissue. Serving as a positive control for ketogenic FA-metabolism, *sirt3* and *pparγ2* expression occurred in ketogenic diet fed mice according to literature for HFD and ketogenic diets (Miller et al 2018, Lima et al 2019). The upregulation of *ucp3* in liver, which was not reported so far under fasting conditions in mice, was observed and is in line with the increased *ppargγ2* expression, that is documented to be a transcription factor of *ucp3* (Lima et al 2019).

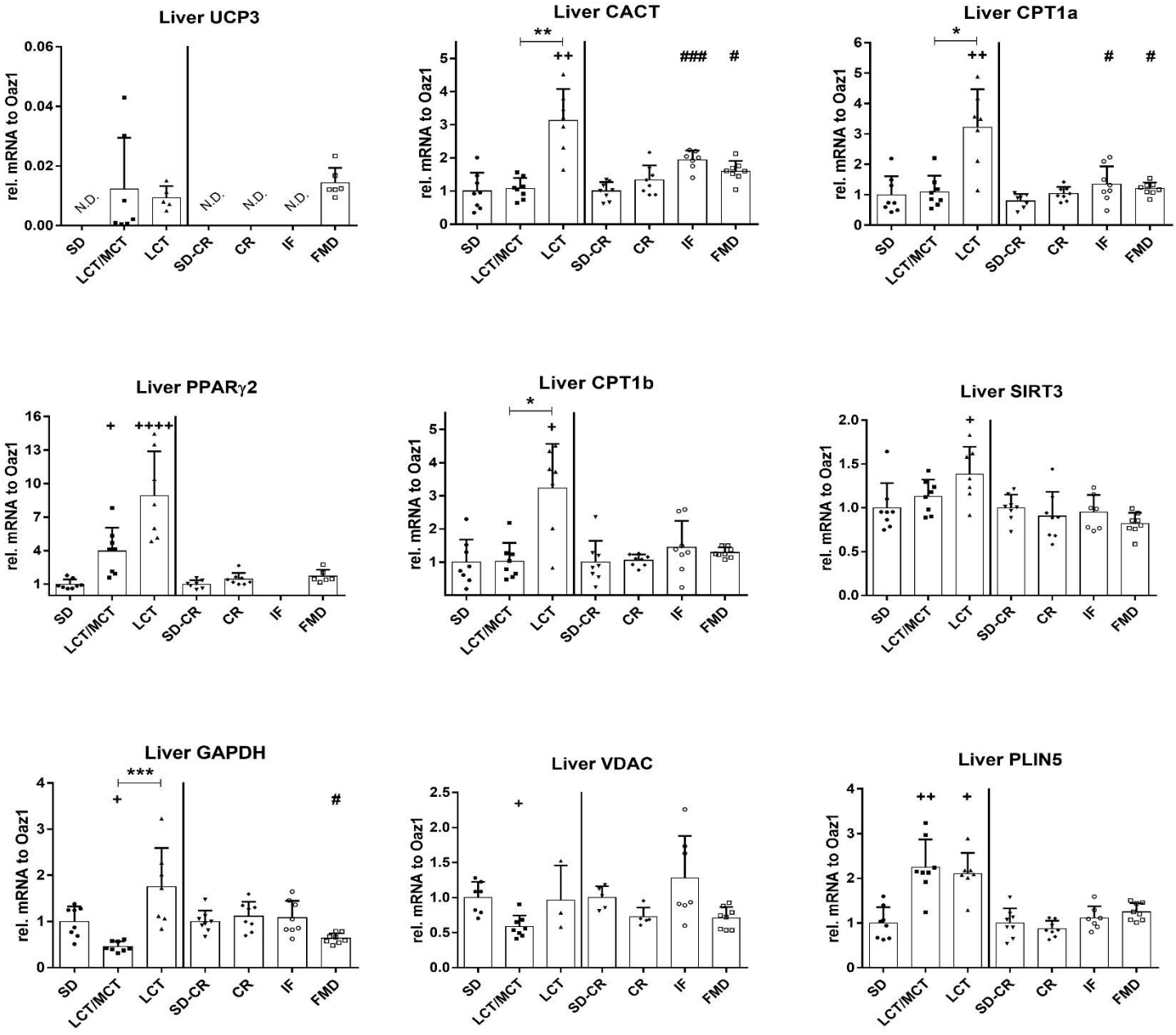

Figure 4.8 ***Molecular mRNA expression in LCT/MCT, LCT, CR, IF and FMD to the respective control diet (SD or SD-CR) in murine liver tissue.*** *Relative mRNA levels of ucp3, cact, cpt1a, cpt1b, pparγ2, glut4, plin5, sirt3, gapdh and vdac normalized towards oaz1. All values are depicted as mean ± SD, n = 7-8 mice per group, one-way ANOVA and Dunn's multiple comparison, non-parametric Kruskal-Wallis. SD tested against LCT/MCT and LCT: significant differences (P-values) marked with + P ≤ 0.05, ++ P ≤ 0.01, +++ P ≤ 0.001 and ++++ P ≤ 0.0001, LCT/MCT tested against LCT: significant differences marked with * P ≤ 0.05, ** P ≤ 0.01, *** P ≤ 0.001 and **** P ≤ 0.0001, SD-CR tested against CR, IF and FMD: significant differences marked with: # P ≤ 0.05, ## P ≤ 0.01, ### P ≤ 0.001 and #### P ≤ 0.0001. LCT, long chain triglycerides; LCT/MCT, long and medium chain triglycerides; SD, standard diet; SD-CR, standard diet calorie restricted; CR, calorie restricted; IF, intermitted fasting; FMD, fasting mimicking diet; n.d., not detectable.*

5. Discussion

Recent literature indicates a role of UCP3 in FA transport and FAO. However, these experiments were mainly performed in rats and mice fed HFD and there is no data on the regulation of *ucp3* in mice upon ketogenic diet feeding. In addition, we wanted to clarify if the diet composition is influencing *ucp3* gene expression under ketogenic settings as previously reported for MCT and LCT fed mice in HFD (Montgomery et al 2013; Wang et al 2018; Murray et al 2011). Our ketogenic diets consisted mainly of triglycerides (LCT and MCT) with moderate protein content and very low carbohydrates (Table 3.4), with either LCT or LCT plus MCT (LCT/MCT) in a ratio of 2/3 LCT and 1/3 MCT. Furthermore, we evaluated different fasting conditions as reference conditions for *ucp3* regulation such as FMD (reduced energy amount plant based, "newer" CR diet), IF (24h/24h cycling) and CR (30% reduction in calories – "classical" CR diet) (see Tables 3.4 and 3.5). We expected a regulation of genes involved in FAO upon ketogenic diet feeding (*cpt1a, cpt1b, cact, sirt3, pparγ2*) and lipid handling (*plin5*) and an inverse regulation of genes involved in carbohydrate metabolism (*glut4*). In addition, we expected to see higher *ucp3* levels in mice fed ketogenic LCT then LCT/MCT diets as this MCT effect was reported previously for HFD feeding (Hoeks et al 2003; Murray et al 2011) and because MCT derived C8/C10 FA can pass freely over the mitochondrial membrane but LCT derived C18 FA need active transportation (if we assume that UCP3 is involved in FA transport also). Furthermore, we expected that the carnitine translocase machinery (consisting of CACT, CPT1a, CPT1b) is higher upregulated in tissues of mice fed LCT then LCT/MCT.

As described in literature (Hilse et al 2016), we have observed expression of *ucp3* mRNA expression in BAT, heart and SkM. In accordance to previously published results *pparγ2* mRNA correlates with *ucp3* mRNA upregulation. This is of importance as *pparγ2* was shown to regulate *ucp3* gene expression upstream (Lima et al 2019). We observe the same coupled upregulation of *ucp3* and *pparγ2* in BAT, SkM and heart, but also in liver, that is classically not an *ucp3* expression site. The extent of *ucp3's* regulation was influenced by diet type and respective fasting conditions. In general, both ketogenic diets upregulated *ucp3* expression similar to the reported regulation under HFD (Fisler and Warden 2006). Organ specific changes in FAO and lipid handling related transcripts are in line with literature regarding ketogenic diets

except the finding that the LCT/MCT diets upregulated *ucp3* mRNA more strongly in all organs analysed. This is very intriguing as MCT are proposed to be able to freely pass the IMM (Bach and Babayan 1982, Fritz 1963). It was shown that LCT's upregulate *ucp3* more than MCT's, yet their findings lack a proper mitochondrial normalization strategy – making it hard to put the increased *ucp3* protein content into perspective (Murray et al 2011). Later another paper documented increased UCP3 protein content in mice fed MCT, however the supplemented food's fat content (45 %) was derived from either coconut oil (medium chain FA) or lard (long chain FA). The additional 35 % of carbohydrates confirms, that the mice were in no ketogenic state (Montgomery et al 2013). A recent paper showed an MCT-mediated increase of mitochondrial biogenesis (Wang et al 2018), although the authors proved this only indirectly via genetic upstream pathways involved in mitochondrial biogenesis. This is important as our increased levels of *ucp3* may result from more mitochondria present in the analysed tissues due to mitochondrial-, MCT driven- biogenesis. Of note, unpublished data from our lab (transmission electron microscopy analysis) indicates that mitochondrial amount at least in the heart seems to be unchanged between LCT and LCT/MCT. Parallel to this a weaker upregulation of the carnitine translocase members *cact*, *cpt1a* and *cpt1b,* would have been expected to occur in LCT/MCT compared to LCT which was not the case. Carnitine translocase members are regularly responsible for the translocation of LCT-derived FA into the mitochondria (Kerner and Hoppel 2000). Additionally, we confirmed the expected correlation of *plin5* mRNA levels, which is an indicator for LD present in the cells, and *ucp3.* This gives us indications about LD-mitochondria-UCP3 interactions as suggested by Hilse and colleagues recently (Hilse et al 2018).

To our surprise, we detected a regulation of *vdac* mRNA expression in dependence of the diets fed, especially in oxidative tissue (BAT, heart, SkM). Interestingly, VDAC was also described to be involved in FA transport together with CPT1 (Caterino et al 2017), which would support our findings. Moreover, it was recently reported (Bazhan et al 2019) that *glut4* is decreasing with high concentrations of FA, which is in line with our data regarding LCT-fed mice in all tissues and which was abolished upon MCT addition.

Furthermore, we were interested in comparison of effects of short (IF, 24h) and long-term (CR) caloric restriction on the expression of *ucp3* and related FAO and lipid handling genes.

The strongest effects in terms of metabolic relevant genes changed had the IF regimen thereby adding additional molecular evidence to the current 8/16-lifestyle-hype (humans which eat 8 hours and starve 16 hours). Intriguingly the effect of the IF diet, relating to *gapdh* and *glut4,* proposes that whilst being in an intermitted fasting cycle, the organism finds a balance between gluconeogenesis and β-oxidation at least in BAT. Heart increases its expresseion of both members of the carnitine transferase pathway as well as *glut4* and *gapdh* during IF to keep the energy uptake high, which is in line with the description of the heart as a carnivore.

Very interestingly, we observed minor levels of *ucp3* mRNA in the liver of mice fed LCT, LCT/MCT and FMD. Recent literature does not indicate the liver as *ucp3* expression site (Pohl et al 2019). However, ratios under 0.01 towards *gapdh* are known to result in no protein expression at least for *ucp4* (Rupprecht et al 2014), what can possibly be translated to *ucp3.* In our case the ratio ranges from 0.0007 to 0.0034 for liver tissue. Investigation of UCP3 at protein level is necessary. Interestingly, *ucp3* expression was observed in mice fed HFD (Camara et al 2009). It is worth to mention, that due to our extraction method we cannot differentiate between hepatocytes, fibroblasts, cells of the immune system and others in liver. Thus, as a next step the isolation of primary hepatocyte cultures is required for the correct investigation of UCP3 expression.

In conclusion, our findings support our initial hypothesis that *ucp3* coincides with markers of FAO under a ketogenic diet. In addition, we could clarify that *ucp3* is upregulated similar in a ketogenic-HFD and in an HFD condition (as reported previously). However, our results regarding *ucp3* mRNA expression under MCTs in murine heart, BAT and SkM contradict previous reports (Murray et al 2011; Montgomery et al 2013). However, the diets fed differed significantly compared to our study (non-ketogenic, pure MCT diets) (Montgomery et al 2013) and the normalization strategy used (Murray et al 2011) to determine UCP3 protein amounts make a direct comparison rather difficult.

Interestingly, IF has a similar effect on *ucp3* expression in heart and BAT tissue as ketogenic diets. Our conclusion is based on *ucp3* mRNA expression in heart, liver, SkM and BAT of mice being fed different types of ketogenic diets (LCT and LCT/MCT) or fasting

conditions (FMD, IF and CR), which were compared to respective SD (ketogenic) and SD-CR (fasting) diets.

In summary, we revealed that *ucp3* mRNA is upregulated also under a ketogenic environment and that the type of fatty acid inside the diet is influencing its expression.
Finally, we want to emphasize that the differential gene expression patterns of *ucp3* upon LCT and LCT/MCT feeding have to be validated on the protein level. Future research should also focus on the amount of mitochondria present in the tissues examined in order to set *ucp3* levels into perspective.

6. Summary

Obesity is a growing problem of the 21st century that is affecting millions of people worldwide. Mitochondrial uncoupling protein 3 (UCP3) is proposed to be involved in obesity pathogenesis. It is highly expressed in brown adipose tissue (BAT), skeletal muscle (SkM) and heart tissue. Although the exact function of the protein is not known, it was shown that UCP3's expression correlates with the type of metabolism in the cell. High concentrations of free fatty acids (FA) in the bloodstream and access to high amounts of triglycerides induce FA β-oxidation (FAO) and ketone body utilization. Ketone bodies provide a glucose-independent metabolic pathway that may regulate UCP3's abundance. We hypothesize that the gene expression of UCP3 and other important genes involved in lipid handling in the named tissues show different patterns based upon qualitative changes in the food uptake due to its intervention with the cell metabolism. To analyse these patterns mice were fed different types ketogenic diets and fasting, which, compared to each other, will give us a further hint for UCP3's involvement in the metabolic pathway.

To investigate our hypothesis, C57BL/6NRj mice were fed with different types of diets or held under fasting conditions (caloric restriction-, long chain triglycerides (LCT-) and LCT/medium chain triglycerides (MCT-), intermittent fasting-, fasting mimicking-). These diets were compared to standard and standard calorie restricted diets. Due to *ucp3's* high abundance in tissues relaying on FA oxidation: BAT, SkM and heart tissue and liver as a control tissue, normally not expressing UCP3, were analysed. We used RT-qPCR to analyse the gene expression patterns of *ucp3*, it's transcription factor (*pparγ2*), translocases (*cact*, *glut4, plin5*) and transferases (*cpt1a, cpt1b*), that are involved in FAO, but also further proteins (*sirt3, gapdh, oaz1, actb, vdac, rpl4*) as controls for gene expression and ketosis.

Our results supported our initial hypothesis that *ucp3* expression coincides with markers of FAO under a ketogenic environment but showed the opposite effect on *ucp3* expression under MCT, which contrasts with that described in literature. The results gave an insight in *ucp3* expression, which was regulated similarly in fasting conditions (IF) and ketogenic diets (LCT and LCT/MCT). We also observed a low increase in expression of *ucp3* in liver tissue in ketogenic diets but also in fasting conditions (FMD), even though liver is not a regular

expression site of *ucp3*. We cannot fully rely merely on mRNA data, because of posttranscriptional regulations and mRNA degradation, thus further experiments on protein levels will be performed in the future to confirm these observations. The expression of *ucp3* in liver tissue might be analysed in future studies with FACS, to evaluate its presence in hepatocytes, using similar diets, giving further insight on research of UCP3.

7. Zusammenfassung

Fettleibigkeit ist ein zunehmend wachsendes Problem des 21. Jahrhunderts, von dem weltweit Millionen von Menschen betroffen sind. Es wird postuliert, dass das mitochondriale Entkopplungsprotein 3 (UCP3) an der Pathogenese von Adipositas beteiligt ist. Es wird stark in braunem Fettgewebe (BAT), Skelettmuskel (SkM) und Herzgewebe exprimiert. Obwohl die genaue Funktion des Proteins noch nicht bekannt ist, wurde gezeigt, dass die Expression von UCP3 mit der Art des Metabolismus in der Zelle korreliert. Hohe Konzentrationen an freien Fettsäuren (FA) im Blutkreislauf und der Zugang zu hohen Mengen an Triglyceriden induzieren die β-Oxidation (FAO) und die Ketonkörper-Verwertung. Ketonkörper bieten einen Glucose unabhängigen Stoffwechselweg, der die UCP3-Häufigkeit regulieren kann. Wir nehmen an, dass die Genexpression von UCP3 und anderer wichtiger Gene, die an der Lipidverarbeitung in den genannten Geweben beteiligt sind, unterschiedliche Muster zeigen, die auf der qualitativen Veränderungen in der Nahrungsaufnahme aufgrund ihrer Intervention im Zellstoffwechsel beruhen. Um diese Muster zu analysieren wurden Mäuse mit verschiedenen Arten von ketogenen Diäten gefüttert und verschiedenen Fastenzuständen ausgesetzt, was uns im Vergleich zueinander einen weiteren Hinweis auf die Beteiligung von UCP3 am Stoffwechsel geben kann.

Um unsere Hypothese zu untersuchen wurden C57BL/6NRj-Mäuse mit verschiedenen Arten von Diäten gefüttert oder unter Fastenbedingungen (Kalorienrestriktion, langkettige Triglyceride (LCT) und LCT / mittelkettige Triglyceride (MCT), intermittierendes Fasten und Fastennachahmung) gehalten. Diese Diäten wurden mit Standarddiäten und kalorienreduzierten Standarddiäten verglichen. Aufgrund des hohen Vorhandenseins von UCP3 in Geweben, die auf β-Oxidation beruhen, wurden BAT, SkM und Herzgewebe sowie Leber als Kontrollgewebe, welches normalerweise kein UCP3 exprimiert, analysiert. Wir verwendeten RT-qPCR, um die Genexpressionsmuster von *ucp3*, dessen Transkriptionsfaktor (*pparγ2*), Translokasen (*cact*, *glut4*, *plin5*) und Transferasen (*cpt1a*, *cpt1b*) zu analysieren, die an FAO beteiligt sind, aber auch weitere Proteine (*sirt3*, *gapdh*, o*az1*, *actb*, v*dac*, r*pl4*) als Kontrollen für die Genexpression und Ketose.

Unsere Ergebnisse belegen unsere anfängliche Hypothese, dass die *ucp3*-Expression mit den FAO-Markern in einer ketogenen Umgebung übereinstimmt. Es wird jedoch der gegenteilige Effekt auf die *ucp3*-Expression unter MCT gezeigt, der zu diesem Thema in der Literatur beschriebenen wird. Die Ergebnisse gaben einen Einblick, dass die *ucp3*-Expression beim intermittierenden Fasten ähnlich Resultate liefert wie bei ketogenen Diäten (LCT und LCT / MCT). Wir beobachteten auch einen geringen Anstieg der Expression von *ucp3* im Lebergewebe bei ketogenen Diäten, aber auch bei der Fastennachahmeden Diät (FMD), obwohl die Leber kein regulärer Expressionsort von *ucp3* ist. Aufgrund von post-transkriptionellen Regulationen und mRNA-Abbau, können wir uns nicht vollständig auf mRNA-Daten verlassen. In der Zukunft werden daher weitere Experimente zu Protein Expression durchgeführt, um diese Daten zu bestätigen. Die Expression von *ucp3* im Lebergewebe könnte in zukünftigen Studien mit FACS analysiert werden, um das Vorhandensein von *ucp3* in Hepatozyten unter Verwendung ähnlicher Diäten zu bewerten, um weitere Einblicke in die Erforschung von UCP3 zu erhalten.

8. Abbreviations

Skeletal muscle	SkM
Brown adipose tissue	BAT
Fatty acids	FA
Fatty acid oxidation	FAO
High fatty diet	HFD
Anaplastic lymphoma kinase	ALK
Lipid droplet	LD
Outer mitochondrial membrane	OMM
Inner mitochondrial membrane	IMM
Standard diet	SD
Standard diet calorie restricted	SD-CR
Intermitted fasting	IF
Fasting mimicking diet	FMD
Long chain triglycerides	LCT
Medium chain triglycerides	MCT
Nuclease free water	NF-H_2O
No template control	NTC
Reverse transcription control	RT-
Melting Temperature	Tm
Cycle of quantification	ct
Housekeeping gene	HKG
Uncoupling protein 3	*ucp3*
Carnitine-acylcarnitine-translocase	*cact*
Carnitine palmitoyl transferase 1a	*cpt1a*
Carnitine palmitoyl transferase 1b	*cpt1b*
Glucose transporter type 4 (/Solute carrier family 2 member 4)	*glut4 /slc2a4*
Peroxisome proliferative activated receptor gamma	*pparγ*
Ribosomal protein L4	*rpl4*
Sirtuin 3	*sirt3*
Glyceraldehyde-3-phosphate dehydrogenase	*gapdh*
Ornithine decarboxylase antizyme 1	*oaz1*
Actin beta	*actβ*
Voltage dependent anion carrier	*vdac*
Perilipin 5	*plin5*

9. Tables and Figures

9.1 Tables

9.2 Figures

efficiency test RT-qPCR data. Tm of UCP3 matches our requirements for the Tm of UCP3's RT-qPCR melting temperature test (left). Plotting the ct values against the logarithm of the dilution series (see 3.2.5) and fitting a regression line, calculates the slope from which the efficiency of UCP3 was determined (Table 3.3)(right).

4.5 Figure 4.5 Molecular mRNA expression in LCT/MCT, LCT, CR, IF and FMD to the respective control diet (SD or SD-CR) in murine brown adipose tissue (BAT). Relative mRNA levels of ucp3, cact, cpt1a, cpt1b, pparγ2, glut4, plin5, sirt3, gapdh and vdac normalized towards rpl4. All values are depicted as mean ± SD, n = 7-8 mice per group, one-way ANOVA and Dunn's multiple comparison, non-parametric Kruskal-Wallis. SD tested against LCT/MCT and LCT: significant differences (P-values) marked with + $P \leq 0.05$, ++ $P \leq 0.01$, +++ $P \leq 0.001$ and ++++ $P \leq 0.0001$, LCT/MCT tested against LCT: significant differences marked with * $P \leq 0.05$, ** $P \leq 0.01$, *** $P \leq 0.001$ and **** $P \leq 0.0001$, SD-CR tested against CR, IF and FMD: significant differences marked with: # $P \leq 0.05$, ## $P \leq 0.01$, ### $P \leq 0.001$ and #### $P \leq 0.0001$. LCT, long chain triglycerides; LCT/MCT, long and medium chain triglycerides; SD, standard diet; SD-CR, standard diet calorie restricted; CR, calorie restricted; IF, intermitted fasting; FMD, fasting mimicking diet.

4.6 Molecular mRNA expression in LCT/MCT, LCT, CR, IF and FMD to the respective control diet (SD or SD-CR) in murine heart tissue. Relative mRNA levels of ucp3, cact, cpt1a, cpt1b, pparγ2, glut4, sirt3, plin5, gapdh and vdac normalized towards rpl4. All values are depicted as mean ± SD, n = 7-8 mice per group, one-way ANOVA and Dunn's multiple comparison, non-parametric Kruskal-Wallis. SD tested against LCT/MCT and LCT: significant differences (P-values) marked with + $P \leq 0.05$, ++ $P \leq 0.01$, +++ $P \leq 0.001$ and ++++ $P \leq 0.0001$, LCT/MCT tested against LCT: significant differences marked with * $P \leq 0.05$, ** $P \leq 0.01$, *** $P \leq 0.001$ and **** $P \leq 0.0001$, SD-CR tested against CR, IF and FMD: significant differences marked with: # $P \leq 0.05$, ## $P \leq 0.01$, ### $P \leq 0.001$ and #### $P \leq 0.0001$. LCT, long chain triglycerides; LCT/MCT, long and medium chain triglycerides; SD, standard diet; SD-CR, standard diet calorie restricted; CR, calorie restricted; IF, intermitted fasting; FMD, fasting mimicking diet.

4.7 Molecular mRNA expression in LCT/MCT, LCT, CR, IF and FMD to the respective control diet (SD or SD-CR) in murine skeletal muscle (SKM) tissue. Relative mRNA levels of ucp3, cact, cpt1a, cpt1b, pparγ2, glut4, sirt3, plin5, gapdh and vdac normalized towards rpl4. All values are depicted as mean ± SD, n = 7-8 mice per group, one-way ANOVA and Dunn's multiple comparison, non-parametric Kruskal-Wallis. SD tested against LCT/MCT and LCT: significant differences (P-values) marked with + $P \leq 0.05$, ++ $P \leq 0.01$, +++ $P \leq 0.001$ and ++++ $P \leq 0.0001$, LCT/MCT tested against LCT: significant differences marked with * $P \leq 0.05$, ** $P \leq 0.01$, *** $P \leq 0.001$ and **** $P \leq 0.0001$, SD-CR tested against CR, IF and FMD: significant differences marked with: # $P \leq 0.05$, ## $P \leq 0.01$, ### $P \leq 0.001$ and #### $P \leq 0.0001$. LCT, long chain triglycerides; LCT/MCT, long and medium chain triglycerides; SD, standard diet; SD-CR, standard diet calorie restricted; CR, calorie restricted; IF, intermitted fasting; FMD, fasting mimicking diet.

4.8 Molecular mRNA expression in LCT/MCT, LCT, CR, IF and FMD to the respective control diet (SD or SD-CR) in murine liver tissue. Relative mRNA levels of ucp3, cact, cpt1a, cpt1b, pparγ2, glut4, plin5, sirt3, gapdh and vdac normalized towards oaz1. All values are depicted as mean ± SD, n = 7-8 mice per group, one-way ANOVA and Dunn's multiple comparison, non-parametric Kruskal-Wallis. SD tested against LCT/MCT and LCT: significant differences (P-values) marked with + $P \leq 0.05$, ++ $P \leq 0.01$, +++ $P \leq 0.001$ and ++++ $P \leq 0.0001$, LCT/MCT tested against LCT: significant differences marked with * $P \leq 0.05$, ** $P \leq 0.01$, *** $P \leq 0.001$ and **** $P \leq 0.0001$, SD-CR tested against CR, IF and FMD: significant differences marked with: # $P \leq 0.05$, ## $P \leq 0.01$, ### $P \leq 0.001$ and #### $P \leq 0.0001$. LCT, long chain triglycerides; LCT/MCT, long and medium chain triglycerides; SD, standard diet; SD-CR, standard diet calorie restricted; CR, calorie restricted; IF, intermitted fasting; FMD, fasting mimicking diet; n.d., not detectable.

4 Literature

Alán, K. Smolková, E. Kronusová, J. Šantorová, and P. Ježek, “Absolute levels of transcripts for mitochondrial uncoupling proteins UCP2, UCP3, UCP4, and UCP5 show different patterns in rat and mice tissues,” *J. Bioenerg. Biomembr.*, vol. 41, no. 1, pp. 71–78, 2009.

Alberts et al., "Molecular Biology of the cell (6th edition)," *Garl. sci.,* pp. 753–763, 2015.

Bach and K. Babayan, “Medium-chain triglycerides :,” no. January, pp. 950–962, 2018.

Ballinger and M. T. Andrews, “Nature’s fat-burning machine: Brown adipose tissue in a hibernating mammal,” *J. Exp. Biol.*, vol. 121, 2018.

Bazhan *et al.*, “Sex Differences in Liver, Adipose Tissue, and Muscle Transcriptional Response to Fasting and Refeeding in Mice,” *Cells*, vol. 8, no. 12, p. 1529, 2019.

Benador, M. Veliova, M. Liesa, and O. S. Shirihai, “Mitochondria Bound to Lipid Droplets: Where Mitochondrial Dynamics Regulate Lipid Storage and Utilization,” *Cell Metab.*, vol. 29, no. 4, pp. 827–835, 2019.

Bosch, R. G. Parton, and A. Pol, “Lipid droplets, bioenergetic fluxes, and metabolic flexibility,” *Semin. Cell Dev. Biol.*, no. February, pp. 0–1, 2020.

Bouillaud, D. Ricquier, J. Thibault, and J. Weissenbach, “Molecular approach to thermogenesis in brown adipose tissue: cDNA cloning of the mitochondrial uncoupling protein,” *Proc. Natl. Acad. Sci. U. S. A.*, vol. 82, no. 2, pp. 445–448, 1985.

Bouillaud, “Mitochondrial uncoupling proteins,” *Hear. Metab.*, no. 48, pp. 32–34, 2010.

Camara, T. Mampel, J. Armengol, F. Villarroya, and L. Dejean, “UCP3 Expression in liver modulates gene expression and oxidative metabolism in response to fatty Acids, and sensitizes mitochondria to permeability transition,” *Cell. Physiol. Biochem.*, vol. 24, no. 3–4, pp. 243–252, 2009.

Caterino, M. Ruoppolo, A. Mandola, M. Costanzo, S. Orrù, and E. Imperlini, “Protein-protein interaction networks as a new perspective to evaluate distinct functional roles of voltage-dependent anion channel isoforms,” *Mol. Biosyst.*, vol. 13, no. 12, pp. 2466–2476, 2017.

Cypess *et al.*, “Identification and importance of brown adipose tissue in adult humans,” *Obstet. Gynecol. Surv.*, vol. 64, no. 8, pp. 519–520, 2009.

Dąbek, M. Wojtala, L. Pirola, and A. Balcerczyk, “Modulation of cellular biochemistry, epigenetics and metabolomics by ketone bodies. Implications of the ketogenic diet in the physiology of the organism and pathological states,” *Nutrients*, vol. 12, no. 3, 2020.

de Jonge *et al.*, “Evidence based selection of housekeeping genes,” *PLoS One*, vol. 2, no. 9, pp. 1–5, 2007.

Devarshi, S. M. McNabney, and T. M. Henagan, “Skeletal muscle nucleo-mitochondrial crosstalk in obesity and type 2 diabetes,” *Int. J. Mol. Sci.*, vol. 18, no. 4, 2017.

Finkelstein *et al.*, “Obesity and severe obesity forecasts through 2030,” *Am. J. Prev. Med.*, vol. 42, no. 6, pp. 563–570, 2012.

Fisler and C. H. Warden, “Uncoupling proteins, dietary fat and the metabolic syndrome,” *Nutr. Metab.*, vol. 3, no. July, pp. 1–7, 2006.

Fritz, *Carnitine and Its Role in Fatty Acid Metabolism.*, vol. 64. ACADEMIC PRESS INC., 1963.

Hilse *et al.*, “The expression of UCP3 directly correlates to UCP1 abundance in brown adipose tissue,” *Biochim. Biophys. Acta - Bioenerg.*, vol. 1857, no. 1, pp. 72–78, 2016.

Hilse *et al.*, “The expression of uncoupling protein 3 coincides with the fatty acid oxidation type of metabolism in adult murine heart,” *Front. Physiol.*, vol. 9, no. JUN, pp. 1–11, 2018.

Himms Hagen, “Obesity may be due to a malfunctioning of brown fat,” *Can. Med. Assoc. J.*, vol. 121, no. 10, pp. 1361–1364, 1979.

Hoeks, M. K. C. Hesselink, and P. Schrauwen, “Involvement of UCP3 in mild uncoupling and lipotoxicity,” *Exp. Gerontol.*, vol. 41, no. 7, pp. 658–662, 2006.

Janovick-Guretzky, H. M. Dann, D. B. Carlson, M. R. Murphy, J. J. Loor, and J. K. Drackley, “Housekeeping gene expression in bovine liver is affected by physiological state, feed intake, and dietary treatment,” *J. Dairy Sci.*, vol. 90, no. 5, pp. 2246–2252, 2007.

Kerner and C. Hoppel, “Fatty acid import into mitochondria,” *Biochim. Biophys. Acta - Mol. Cell Biol. Lipids*, vol. 1486, no. 1, pp. 1–17, 2000.

Kuramoto *et al.*, “Perilipin 5, a lipid droplet-binding protein, protects heart from oxidative burden by sequestering fatty acid from excessive oxidation,” *J. Biol. Chem.*, vol. 287, no. 28, pp. 23852–23863, 2012.

Lima *et al.*, “Essential role of the PGC-1α/PPARβ axis in Ucp3 gene induction,” *J. Physiol.*,

vol. 597, no. 16, pp. 4277–4291, 2019.

Macher, M. Koehler, A. Rupprecht, J. Kreiter, P. Hinterdorfer, and E. E. Pohl, “Inhibition of mitochondrial UCP1 and UCP3 by purine nucleotides and phosphate,” *Biochim. Biophys. Acta - Biomembr.*, vol. 1860, no. 3, pp. 664–672, 2018.

Martin and R. G. Parton, “a Dynamic Organelle,” *Mol. Cell*, vol. 7, no. May, pp. 373–378, 2006.

Mason and M. J. Watt, “Unraveling the roles of PLIN5: Linking cell biology to physiology,” *Trends Endocrinol. Metab.*, vol. 26, no. 3, pp. 144–152, 2015.

Miller, F. A. Villamena, and J. S. Volek, “Nutritional ketosis and mitohormesis: Potential implications for mitochondrial function and human health,” *J. Nutr. Metab.*, vol. 2018, 2020.

Montgomery *et al.*, “Contrasting metabolic effects of medium-versus long-chain fatty acids in skeletal muscle,” *J. Lipid Res.*, vol. 54, no. 12, pp. 3322–3333, 2013.

Moschinger *et al.*, “Age-related sex differences in the expression of important disease-linked mitochondrial proteins in mice,” *Biol. Sex Differ.*, vol. 10, no. 1, pp. 1–10, 2019.

Murray, N. S. Knight, S. E. Little, L. E. Cochlin, M. Clements, and K. Clarke, “Dietary long-chain, but not medium-chain, triglycerides impair exercise performance and uncouple cardiac mitochondria in rats,” *Nutr. Metab.*, vol. 8, pp. 1–9, 2011.

Nedergaard and B. Cannon, “The ‘novel’ ‘uncoupling’ proteins UCP2 and UCP3: what do they really do? Pros and cons for suggested functions.,” *Exp. Physiol.*, vol. 88, no. 1, pp. 65–84, 2003.

Nedergaard, V. Golozoubova, A. Matthias, A. Asadi, A. Jacobsson, and B. Cannon, “UCP1: the only protein able to mediate adaptive non-shivering thermogenesis and metabolic ineffciency,” *Bioch. et Biophy. Acta* vol. 1504, pp. 82–106, 2001.

Nicholls, “The hunt for the molecular mechanism of brown fat thermogenesis,” *Biochimie*, vol. 134, pp. 9–18, 2017.

Ochoa *et al.*, “Association between obesity and insulin resistance with UCP2-UCP3 gene variants in Spanish children and adolescents,” *Mol. Genet. Metab.*, vol. 92, no. 4, pp. 351–358, 2007.

Orthofer *et al.*, “Identification of ALK in Thinness,” *Cell*, vol. 181, no. 6, pp. 1–17, 2020.

Palmieri, “The mitochondrial transporter family (SLC25): Physiological and pathological

implications," *Pflugers Arch. Eur. J. Physiol.*, vol. 447, no. 5, pp. 689–709, 2004.

Pohl, A. Rupprecht, G. Macher, K. E. Hilse, and D. Richard, "Important Trends in UCP3 Investigation," vol. 10, no. April, pp. 1–16, 2019.

Ramsden *et al.*, "Human neuronal uncoupling proteins 4 and 5 (UCP4 and UCP5): Structural properties, regulation, and physiological role in protection against oxidative stress and mitochondrial dysfunction," *Brain Behav.*, vol. 2, no. 4, pp. 468–478, 2012.

Ricquier and F. Bouillaud, "The uncoupling protein homologues: UCP1, UCP2, UCP3, StUCP and AtUCP," *Biochem. J.*, vol. 345, no. 2, pp. 161–179, 2000.

Riley *et al.*, "The complementary and divergent roles of uncoupling proteins 1 and 3 in thermoregulation," *J. Physiol.*, vol. 594, no. 24, pp. 7455–7464, 2016.

Roberts *et al.*, "A Ketogenic Diet Extends Longevity and Healthspan in Adult Mice," *Cell Metab.*, vol. 26, no. 3, pp. 539-546.e5, 2017.

Rousset *et al.*, "The Biology of Mitochondrial Uncoupling Proteins," *Diabetes*, vol. 53, no. SUPPL. 1, 2004.

Rupprecht *et al.*, "Uncoupling protein 2 and 4 expression pattern during stem cell differentiation provides new insight into their putative function," *PLoS One*, vol. 9, no. 2, pp. 1–10, 2014.

Russell *et al.*, "UCP3 protein expression is lower in type I, IIa and IIx muscle fiber types of endurance-trained compared to untrained subjects," *Pflugers Arch. Eur. J. Physiol.*, vol. 445, no. 5, pp. 563–569, 2003.

Schrauwen and M. K. C. Hesselink, "The role of uncoupling protein 3 in fatty acid metabolism: protection against lipotoxicity?," *Proc. Nutr. Soc.*, vol. 63, no. 2, pp. 287–292, 2004.

Vidali *et al.*, "Mitochondria: The ketogenic diet - A metabolism-based therapy," *Int. J. Biochem. Cell Biol.*, vol. 63, pp. 55–59, 2015.

Vozza *et al.*, "UCP2 transports C4 metabolites out of mitochondria, regulating glucose and glutamine oxidation," *Proc. Natl. Acad. Sci. U. S. A.*, vol. 111, no. 3, pp. 960–965, 2014.

Wang, Z. Liu, Y. Han, J. Xu, W. Huang, and Z. Li, "Medium Chain Triglycerides enhances exercise endurance through the increased mitochondrial biogenesis and metabolism," *PLoS One*, vol. 13, no. 2, pp. 1–11, 2018.

Žáčkova and P. Ježek, “Reconstitution of novel mitochondrial uncoupling proteins UCP2 and UCP3,” *Biosci. Rep.*, vol. 22, no. 1, pp. 33–46, 2002.

Zhou, P. Mukherjee, M. A. Kiebish, W. T. Markis, J. G. Mantis, and T. N. Seyfried, “The calorically restricted ketogenic diet, an effective alternative therapy for malignant brain cancer,” *Nutr. Metab.*, vol. 4, pp. 1–15, 2007.

Zingaretti *et al.*, “The presence of UCP1 demonstrates that metabolically active adipose tissue in the neck of adult humans truly represents brown adipose tissue,” *FASEB J.*, vol. 23, no. 9, pp. 3113–3120, 2009.